Title: Lon protease: a novel mitochondrial matrix protein in the interconnection between drug-induced mitochondrial dysfunction and ER stress

Authors: Miriam Polo[1,2], Fernando Alegre[1,2], Angela B. Moragrega[1], Lara Gibellini[3], Alberto Marti-Rodrigo[1], Ana Blas-Garcia[1,2,4], Juan V. Esplugues[1,2,4] and Nadezda Apostolova[1,4*]

[1]Departamento de Farmacología, Facultad de Medicina, Universitat de Valencia, Valencia, Spain

[2]FISABIO-Hospital Universitario Doctor Peset, Valencia, Spain

[3]Department of Surgery, Medicine, Dentistry and Morphological Sciences, University of Modena and Reggio Emilia School of Medicine, Modena, Italy

[4]Centro de Investigación Biomédica en Red de Enfermedades Hepáticas y Digestivas (CIBERehd), Valencia, Spain

*Corresponding author

Address: Avda. Blasco Ibáñez n.15–17, 46010 Valencia, Spain.

Tel: (+34) 963983767 Fax: (+34) 963983879

E-mail: nadezda.apostolova@uv.es

Author contributions:

MP, FA, ABM and AM-R performed experiments, analyzed data and prepared the figures; LG analyzed data, prepared figures, critically revised data and critically read the MS; NA, AB-G, JVE designed experiments, critically revised data, drafted and wrote the MS.

This article has been accepted for publication and undergone full peer review but has not been through the copyediting, typesetting, pagination and proofreading process which may lead to differences between this version and the Version of Record. Please cite this article as doi: 10.1111/bph.14045

Keywords: mitochondria, endoplasmic reticulum, MAM, antiretroviral drug, Lon, Efavirenz

Running title: Lon is located to MAMs in drug-induced mitochondrial/ ER stress

Abbreviations: CCCP (carbonyl cyanide m-chlorophenyl hydrazone), Drp1 (dynamin-related protein 1), EFV (efavirenz), ER (endoplasmic reticulum), ETC (electron transport chain), HUVEC (human umbilical vein endothelial cells), IMM (inner mitochondrial membrane), MAMs (mitochondria-associated membranes), Mfn1 (mitofusin 1), Mfn2 (mitofusin 2), MM (mitochondrial matrix), NF-*k*B (nuclear factor- kappa B), OMM (outer mitochondrial membrane), OPA1 (optic atrophy 1), RPV (rilpivirine), TG (thapsigargin), PBS (phosphate buffered saline), VDAC (voltage-dependent anion channel)

Abstract

Background and Purpose. Mitochondria-associated membranes (MAMs) are specific ER-domains that enable direct interaction with mitochondria and mediate metabolic flow and Ca^{2+} transfer. A growing list of proteins have been identified as MAMs components, but how they are recruited and function during complex cell stress situations is still not understood while the participation of mitochondrial matrix proteins is largely undervalued. **Experimental Approach.** This work compares mitochondrial/ER contact during combined ER stress/mitochondrial dysfunction using a model of human hepatoma cells (Hep3B cell line) treated for 24h with classic pharmacological inducers of ER stress (thapsigargin), mitochondrial dysfunction (CCCP or rotenone) or both (the antiretroviral drug Efavirenz used at clinically relevant concentrations). **Key Results.** Markers of mitochondrial dynamics (Drp1, OPA1, Mfn2) were expressed differentially with these stimuli, pointing to a specificity of combined ER/mitochondrial stress. Lon, a matrix protease involved in protein and mtDNA quality control, was upregulated at mRNA and protein levels under all conditions. However, only with efavirenz, the mitochondrial content of Lon was diminished while its

extramitochondrial presence was increased, as did its localization to MAMs, where it enhanced mitochondria/ER interaction as shown by co-immunoprecipitation experiments of MAM protein partners and confocal microscopy imaging. **Conclusion and Implications.** A specific dual drug-induced mitochondria-ER effect enhances MAMs content and extramitochondrial Lon expression. This is the first report of this phenomenon and suggests a novel MAM-linked function of Lon protease.

1. Introduction

The endoplasmic reticulum (ER) is a membrane-bound organelle involved in the synthesis, storing, modifying and transport of newly synthesized proteins, as well as regulation of intracellular Ca^{2+} trafficking (Lodish, *et al.*, 2000). Mitochondria, which also directly participate in cellular Ca^{2+} homeostasis, are subcellular compartments where ATP is generated and where many metabolic pathways take place (tricarboxylic acid cycle, and synthesis of urea and phospholipids (Lodish, *et al.*, 2000). It is well known that the tight functional link between ER and mitochondria is fundamental for the maintenance of cellular homeostasis, which is vital under stress conditions (Giorgi *et al.*, 2009). However, in accordance with the traditional view of these organelles as independent entities, the bulk of the research regarding cell stress mechanisms has focused on either one of these organelles separately. A long list of human pathologies has been related to mitochondrial dysfunction and/or ER-stress, but little is known about the spatio/temporal interconnection between these crucial phenomena. Nevertheless, it may harbor major clinical relevance, for example, mitochondrial changes in response to ER-stress conditions have been described for several human diseases, including type II diabetes and Alzheimer's disease (Vannuvel *et al.*, 2013).

Additionally, in recent years, it has become evident that these two organelles are spatially connected through specific and tightly regulated contact sites known as mitochondria-associated ER membranes (MAMs) (Vance, 1990). The composition and function of these structures are still far from being understood; however, current knowledge suggests that MAMs enable a two-way supply of fundamental metabolites/messengers, such as lipids or Ca^{2+}, while modulating the bioenergetic fate of the cell (Giorgi *et al.*, 2009). Many proteins have been shown to participate in MAM, and it is evident that the composition of these structures adapts in response to multiple internal and external stimuli (Bui *et al.*, 2010). One of the most widely described complexes involves the mitochondrial voltage-dependent anion channel (VDAC) and ER inositol trisphosphate receptor (IP_3R), which physically interact through the chaperone Grp75 (mitochondrial HSP70) (Szabadkai *et al.*, 2006). In addition, abundant evidence points to the fact that the dynamics of both ER and mitochondria depend on the formation and dissolution of ER–mitochondrial contacts. In line with this, it is known that many proteins involved in ER tubule fusion and/or mitochondrial distribution and morphology are either integral components of MAMs or interact with it (Bui *et al.*, 2010). For example, the dynamin-related mitochondrial fusion protein Mfn2, present at both the ER and mitochondrial surface (de Brito and Scorrano, 2008), not only enables intermitochondrial contacts, but also regulates ER shape and ER–mitochondrial tethering. Moreover, the ER has been connected with mitochondrial fission (Friedman *et al.*, 2011), and numerous co-immunoprecipitation experiments have revealed contacts of classic mitochondrial fission mediators (Fis1, Drp1) with typical ER-bound proteins. The relative participation of ER and mitochondria in the fission complex triggered by different stimuli and how it affects the different physipathological outcomes is not yet fully understood. In this regard, the vast majority of mitochondrial proteins thought to be related to MAMs and/or fission are outer membrane (OMM) proteins, while

understanding of the specific connection between inner mitochondrial (IMM)/mitochondrial matrix (MM) proteins and the ER is lacking.

The mitochondrial protein quality control protease Lon is located in the MM (*Hori et al.*, 2002), and has been implicated in numerous processes, including degradation of oxidatively damaged mitochondrial proteins (Bota and Davies, 2002), assembly of electron transport chain (ETC) complexes (Fukuda et al., 2007), and regulation of mtDNA maintenance, transcription and replication (Matsushima *et al.*, 2010). There is mounting evidence that Lon is up-regulated upon ER stress in order to protect mitochondrial function from ER stress-induced damage (Han *et al.*, 2013; Rainbolt *et al.*, 2014). However, unlike other mitochondrial quality control factors located in MM - such as Grp75/HSPA9, which has been related to MAMs and can have extramitochondrial localization -, no clear connection exists regarding Lon and the mitochondria/ER coupling that occurs under stress conditions.

The aim of this work was to compare mitochondrial/ER contact during combined ER/mitochondrial stress using an *in vitro* model and to establish whether Lon is involved in this interorganelle interaction. In previous publications (Apostolova *et al.*, 2013; Polo *et al.*, 2015), we have described an intriguing dual phenomenon of mitochondrial and ER-stress in human hepatic cells treated with the antiretroviral drug Efavirenz. This non-nucleoside analogue RT inhibitor exerts a rapid, direct inhibitory effect on mitochondrial respiration, which leads to a decrease in mitochondrial membrane potential ($\Delta\Psi_m$) and incremented ROS levels (Apostolova *et al.*, 2010; Polo *et al.*, 2015). Secondary to its mitochondrial action, EFV activates UPR and produces ER-stress (Apostolova *et al.*, 2013). Moreover, this dual effect of EFV is associated with up-regulation of Lon expression, an effect that is diminished in cells with compromised mitochondrial respiration (Polo *et al.*, 2015). Having previously analyzed the mitochondrial effect of Efavirenz, we now anticipated that mitochondrial dynamics might be altered and that the expression of fusion/fission proteins might be modified. We compared

this action with those exerted by other pharmacological cellular stressors that interfere with mitochondrial and ER-function and thus display similarities with EFV- thapsigargin (TG), rotenone (Rot) and CCCP. Additionally, many of the proteins involved in mitochondrial dynamics are direct or indirect participants in the MAMs which lead us to analyze MAMs in our model.

The hypothesis of Lon´s participation was based on two observations: 1) Lon is a mitochondrial protein induced by ER stress, and 2) there are reasonable similarities between Lon and Grp75, a notorious MAMs protein. Our results support an association of Lon with MAMs and provides evidence that this relation occurs specifically in a model of dual drug-induced mitochondrial/ER-stress.

2. Materials and methods

2.1 Reagents and Drugs

Unless stated otherwise, general chemical reagents were purchased from Sigma-Aldrich (Steinheim, Germany). Efavirenz (EFV, Sequoia Research Products, Pangbourne, UK); was employed as the reference drug (in methanol, 3 mg/mL) at clinically relevant plasma concentrations (10, 25 and 50μM) which were chosen taking into account the great interindividual varibility in the pharmacokinetics of this drug (Burger *et al.*, 2006; Carr *et al.*, 2010; Gounden *et al.*, 2010). Rilpivirine (RPV, Sequoia Research Products) was dissolved in DMSO (1mM) and employed at clinically relevant plasma concentrations (0.25, 0.5 and 1μM).

2.2 Cell culture, treatments and transfections

Experiments were performed with the human hepatoblastoma cell line Hep3B (ATCC HB-8064), which displays a certain degree of Cytochrome P450 activity (specifically CYP2B6) capable of metabolising EFV (Zhu et al., 2007; Lin et al., 2012). Cells were cultured in minimal essential medium (MEM), supplemented with 10% heat-inactivated foetal bovine serum (FBS),

2mM L-glutamine, 1mM non-essential amino acids, 1mM sodium pyruvate. For comparison, in some experiments, we also employed the human glioma cell line U-251MG (CLS 300385, European Collection of Cell Culture, Salisbury, UK) which was cultured as described previously (Funes et al., 2014) and the primary cell line HUVEC (Human Umbilical Vein Endothelial Cells) which was isolated from fresh human umbilical cords by extraction with collagenase and cultured in EMG-2 medium supplemented with 2.5 μg/mL fungizone-amphotericin B and BulletKit components (Clonetics, Lonza, Walkersville, MD, USA) according to the manufacturer's instructions (Apostolova et al., 2010). The protocol employed complied with European Community guidelines for the use of human experimental models and was approved by the Ethics Committee of the University of Valencia.

Cell cultures were used for experiments at passage number lower than 25 (for Hep3B and U-251MG) or lower than 3 (for HUVEC). All cell cultures were maintained in the presence of penicillin (50 units/mL) and streptomycin (50 μg/mL). Unless stated otherwise, all the reagents employed in cell culture were purchased from ThermoFisher Scientific, Walthman, MA. All cell cultures were maintained in an incubator (IGO 150, Jouan, Saint-Herblain Cedes, France) at 37ºC, in a humidified atmosphere of 5% CO_2/95% air (AirLiquide Medicinal, Valencia, Spain). Treatments were performed for 24h in complete cell culture medium.

To induce NF-κB we used "LPS cocktail" composed of *E. coli* endotoxin LPS (5 μg/mL), IFN-γ (500 U/mL) and TNF-α (25 ng/mL).

To analyze details of Lon´s up-regulation, we used the highly selective PERK inhibitor GSK2656157 (1μM) and the superoxide dismutase/catalase mimetic MnTMPyP (50μM), purchased from Santa Cruz Biotechnology (Heidelberg, Germany) and Calbiochem (San Diego, CA, USA) respectively. In both cases, cells were pretreated for 1h with the corresponding agent and then 24h-treatment was performed without refreshing the medium.

CHOP/DDIT3/GADD153 and *LONP1* transient silencing were achieved with small interfering RNA (siRNA) using SignalSilence® unconjugated control siRNA as a control (Cell Signaling, Danvers, MA, USA). Transient transfection was performed using Lipofectamine™ 2000 according to the manufacturer's instructions (ThermoFisher Scientific). siRNA/Lipofectamine complexes were formed in serum-free OptiMEM using 12.5µL of Lipofectamine™ 2000 and 50 nM of *GADD153 siRNA(h)* from Santa Cruz Biotechnology or 10nM *LONP1 siRNA(h)* from Ambion® (Thermo Fisher Scientific). Transfections were performed in t-25 flasks with complete cell culture medium without antibiotics over 24h (*CHOP)* or 48h (*LONP1)*, and then cells were re-fed with fresh complete medium containing antibiotics. Transfected cells were then treated as indicated above.

2.3 Immunoblotting for assessment of protein expression

Western Blotting (WB) was performed using 50µg of total cell protein extracts, 20µg of mitochondria-enriched extracts or 20µg of cytosolic extract. Lysates were obtained, quantified and immunoblotted as described elsewhere (Apostolova et al., 2010). Primary antibodies: anti-CIV subunit II (mouse monoclonal), anti-FACL4 (rabbit polyclonal) and anti-phospho-PERK Thr981 (rabbit polyclonal) used at 1:1000 from ThermoFisher Scientific; anti-Porin at 1:1000, anti-Lon at 1:1000, anti-PTPIP51 (FAM82A2) at 1:2000, anti-Grp75 at 1:500 (all rabbit polyclonal), anti-ClpX at 1:1000 (rabbit monoclonal), anti-Mitofusin 2 (Mfn2) at 1:1000, anti-Calnexin at 1:1000 (rabbit polyclonal) and anti-CHOP at 1:1000 (mouse monoclonal) from Abcam, Cambridge, UK; anti-Actin (rabbit polyclonal) and anti-Tubulin (mouse monoclonal) at 1:1000 (Sigma-Aldrich); anti-TOM20 at 1:1000 (rabbit polyclonal from Proteintech, Rosemont, IL, USA); rabbit monoclonal anti-Drp1 and rabbit polyclonal anti-phospho-Drp1 (Ser616) at 1:1000 (Cell Signaling, Danvers, MA, USA); anti-OPA1, anti-Cytochrome *c* and anti-IP_3R_3 at 1:1000 (mouse monoclonal antibodies from BD Biosciences, Franklin Lakes, NJ, USA); anti-LDH and anti-VAP B/C (rabbit polyclonal antibodies at 1:1000 from Santa Cruz,

Dallas, TX, USA). Secondary antibodies: peroxidase-labelled anti-mouse at 1:2000 (ThermoFisher Scientific) and anti-rabbit IgG at 1:5000 (Vector laboratories, Burlingame, CA, USA). Inmunolabelling was detected using the chemiluminescent substrate Luminata™ Crescendo or Forte (Merck Millipore, Billerica, MA, USA), and was visualized with a digital luminescent image analyser (FUJIFILM LAS 3000, Fujifilm). Multi Gauge software version 3.0. was used for densitometric analysis.

2.4 Co-immunoprecipitation

Whole-cell protein extracts were obtained using t-150 flask cell cultures, as described elsewhere (Apostolova et al., 2010). For immunoprecipitation, 1mg or 200µg of protein were incubated overnight with polyclonal antibody against PTPIP51 (FAM82A2) (Abcam, Cambridge, UK) or Porin (Proteintech), respectively, under agitation at 4ºC. After binding to protein A-Sepharose CL-4B beads (GE Healthcare, Buckinghamshire, UK) (4h, 4ºC under agitation), immunoprecipitates were washed three times with protein extraction buffer. In order to denature the protein and separate it from the protein-A beads, Laemmli buffer 2X was added and boiled (99ºC, 5min). Finally, samples were centrifugated and supernatants were analyzed by immunoblotting to study VAP B/C-PTPIP51 and Grp75-Porin interactions, for which VAP B/C and Grp75 were immunodetected, as detailed in section 2.3.

2.5 Confocal fluorescence microscopy

Treatment was performed in multi-well coverslips (ThermoFisher Scientific) and where necessary, cells were incubated with 0.5µM MitoView™ 633 (Biotium, Hayward, CA, USA) in the last 30 min of treatment. Then, cells were fixed with 4% formaldehyde (15min, RT), blocked (60min, RT) and incubated (overnight, 4ºC) with primary antibodies: anti-phospho-Drp1 at 1:200 (Cell Signaling, Danvers, MA, USA), anti-TOM20 at 1:250 to mark mitochondria (BD Biosciences, NJ, USA), anti-Calnexin at 1:750 to mark ER (ThermoFisher Scientific) or anti-Lon at 1:50 (Proteintech). Samples were washed and incubated with

secondary antibodies (goat anti-rabbit Alexa Fluor 488 or goat anti-mouse Alexa Fluor 594 from ThermoFisher Scientific, 1h, RT) and 5μM of the fluorochrome Hoechst 33342 was added for the last 30min (to mark nuclei).

After washing with PBS, images were acquired with a Leica TCS-SP2 confocal laser scanning unit with argon and helium-neon laser beams and attached to a Leica DMIRBE inverted microscope. Images were captured at 63x magnification with a HCX PL APO 40.0 x 1.32 oil UV objective. Colocalization analysis was performed with the programme Image J. Technical replicates – duplicates were employed to ensure the reliability of single values.

2.6 Live cells fluorescence microscopy and static cytometry

All treatments were performed in 24-well plates, and then, after a washing step (HBSS), 16–30 images per well were recorded with a fluorescence microscope (IX81, Olympus, Hamburg, Germany) coupled with a static cytometry software 'ScanR' version 2.03.2 (Olympus). Technical replicates – duplicates were employed to ensure the reliability of single values. In order to assess mitochondrial function, specifically $\Delta\Psi m$, superoxide production and mitochondrial mass, the fluorochromes 5μM TMRM, 2.5μM MitoSOX (both from Molecular Probes, Invitrogen) or 1μM NAO ((10-N-nonyl acridine orange, Sigma-Aldrich) were added for the last 30min of treatment. Nuclei were stained with the fluorochrome Hoechst 33342 (2.5 μM, Sigma -Aldrich), also added for the last 30 min of the treatment, and this signal was employed to count nuclei and assess cellular viability/proliferation (Polo *et al.*, 2015).

2.7 Chromatin immunoprecipitation (ChIP) assay

In order to stabilize protein-DNA complexes, treated cell cultures (t-25 flasks) were crosslinked with 1% formaldehyde (RT, 10min) and incubated with 0.125M glycine (RT, 2min). Subsequently, cells were washed three times and collected with ice-cold PBS and then centrifuged (4ºC, 5min, 500g). Pellets were then resuspended in 0.3mL of SDS sonication buffer (1% SDS, 5mM EDTA, 50mM Tris-HCl pH 8.0 and protease inhibitor cocktail (Roche

Diagnostics GmbH, Mannheim, Germany)) and sonicated three times for 20s (40s in between) at maximum speed (Branson Digital Sonifier, Emerson Electric Co., MO, USA). After centrifugation at maximum speed for 10min at 4°C, supernatants (Chip extracts) were collected and immunoprecipitation was performed overnight at 4°C with anti-NF-κB antibody or with control IgG antibody (secondary antibody for anti-NFκB) (both from ThermoFisher Scientific). Supernatants were then incubated with 60µL protein A-Sepharose CL-4B beads (GE Healthcare) overnight at 4°C. Finally, precipitates were washed sequentially for 5min; once with low-salt wash buffer (1% Triton X-100, 2mM EDTA, 20mM Tris-HCl pH 8, 150mM NaCl), twice with high-salt wash buffer (1% Triton X-100, 2mM EDTA, 20mM Tris-HCl pH 8, 500mM NaCl) and once with LiCl wash buffer (0.25mM LiCl, 1% NP-40, 0.1% Tween 20, 1mM EDTA, 10mM Tris-HCl pH 8), 5 min each. Precipitates were then washed twice with TE buffer (10mM Tris-HCl pH 8.0, 1mM EDTA) and extracted twice with elution buffer (1% SDS, 0.1M $NaHCO_3$). To reverse the formaldehyde crosslinking, eluates were pooled and heated at 65°C for 16h in the presence of 0.25M NaCl. DNA fragments were purified with a PureLink™ Quick PCR purification kit (ThermoFisher Scientific) and DNA content was quantified using a NanoDrop® ND-1000 spectrophotometer (NanoDrop Technologies, Wilmington, DE, USA). The same amount of DNA of all the samples was used to perform semiquantitative PCR for which we employed TaKaRa Taq™ (Takara Bio, Kusatsu, Japan) with the following primers: 5'- CCACCAGCATCAACATCAG-3' and 5'-CGCATGCTCAAGATTCAGG-3', detecting the region -121 to -307 in *LONP1* promoter. PCR of 40 cycles was performed using GeneAmp PCR System 2400, (Perkin Elmer, Waltham, MA, USA) and the obtained PCR products were separated by electrophoresis in 2% agarose gel.

2.8 Isolation of mitochondria-associated membranes (MAMs)

Subcellular fractioning - including MAMs isolation - was performed using cell pellets obtained from 12-14 confluent t-150 flasks per condition (untreated cells and cells treated for 24h with EFV 25µM, TG 2µM and CCCP 10µM). Isolation was performed as described by Wieckowski et al., 2009. In brief, cells were homogenized using a Teflon pestle at 4ºC and serial centrifugations (all at 4ºC) were performed to separate cytosolic, ER and mitochondrial fractions. In order to purify MAMs, crude mitochondria were fractionated in Percoll medium by centrifugation at 95,000*g* for 30min at 4°C in a Beckman Coulter Optima L-100 XP Ultracentrifuge with a SW40 rotor (Beckman, Fullerton, CA, USA). Finally, the obtained subcellular protein fractions (0.5-6µg/µL) were analyzed by WB (see section 2.3).

2.9 Quantitative RT-PCR

Real time RT-PCR (in duplicate, to ensure the reliability of single measurements), of at least three independent experiments (n=3), were performed using mRNA of t-25 flask cell cultures treated with vehicles (Methanol or DMSO), EFV (10, 25, 50µM), thapsigargin (TG, 2µM), rotenone (Rot, 25µM) and CCCP10µM. Total RNA was extracted (RNeasy Mini Kit, Qiagen, Hilden, Germany), eluted in 30µl of water and quantified (NanoDrop® ND-1000 spectrophotometer). cDNA was synthetized (SuperScript™ III Reverse Transcriptase, ThermoFisher Scientific) with 1µg of total RNA in a final volume of 20µL. PCR reactions (Carousel-based LightCycler® 2.0 Real Time PCR System, Roche Applied Biosystems) were performed mixing 1µl of cDNA with LightCycler® FastStart DNA MasterPLUS SYBR Green I master mix (Roche Applied Science). Primers: *LONP1*(s) ATGGAGGACGTCAAGAAACG, *LONP*1(as) GATCTCAGCCACGTCAGTCA; *MFN1*(s) ACCGAGGAGGTGGCAAACAAAG, *MFN1*(as) GCTGGGTCTGAAGCACTAAGGC; *MFN2*(s) GGTGCTCAACGCCAGGATTCAG, *MFN2*(as) TGCCGCTCTTCACGCATTTCC; *OPA1*(s) GGCATGGCTCCTGACACAAAGG,

OPA1(as) GCTGAATCCTGCTTGGACTGGC; *FIS1*(s) AAGGGAGCAAGGAGGAACAGCG, *FIS1*(as) ACAGCAAGTCCGATGAGTCCGG; *DRP1*(s) GACTTTGCTGATGCTTGTGGGC, *DRP1*(as) CTCTCCAGTTGCCTGTGGTTGG and *ACTB*(s) GGACTTCGAGCAAGAGATGG, *ACTB*(as) AGCACTGTGTTGGCGTACAG employed as a housekeeping gene (TIB MOLBIOL, Berlin, Germany). All were used at 1µM and were added to a 10µL final reaction volume. The reaction was: 30s-95°C; 5s-95°C, 20s-60ºC (45 cycles); 15s-65°C and 30s-40°C.

2.10 Presentation of data and statistical analysis

1. Data were analysed with GraphPad Prism v.3 software (GraphPad Prism Software, La Jolla, CA, USA). For the comparison between EFV treatments and their vehicle (methanol), on one hand, and the three pharmacological stressors (thapsigargin, rotenone and CCCP) and their vehicle (DMSO), on the other hand, One-way ANOVA was used with Dunnett´s multiple comparison test. In most cases, data are represented as % of control, the negative control (untreated cells) being considered 100%. Such normalization was performed in order to discard any unwanted sources of variation. All values are expressed as a mean±SEM, ."n" number in the figure legends which denotes the number of biological replicates (independent repetitions) used for statistical analysis was at least 5. Statistical significance was considered vs vehicle: Methanol in the case of EFV (*$p<0.05$) and DMSO in the case of RPV, TG, Rot and CCCP ($^{\#}p<0.05$). Technical replicates in a run (at least in duplicate) were averaged and yielded a value for a biological replicate.

The study was performed in vitro using cell lines and all the samples were analyzed/quantified objectively, without randomization of samples or blinding of the operator due to technical limitations and a large number of assays. The data and statistical analyses comply with the recommendations on experimental design and analysis in pharmacology (Curtis et al., 2015).

2.11 Nomenclature of targets and ligands

Key protein targets and/or ligands in this article are hyperlinked to corresponding entries in http://www.guidetopharmacology.org, the common portal for data from the IUPHAR/BPS Guide to PHARMACOLOGY (Southan *et al.*, 2016).

3. Results

3.1 Mitochondrial dynamics is altered differentially in cells presenting dual mitochondrial/ER stress

Firstly, we analyzed the gene and protein expression of several markers of mitochondrial dynamics in cells treated with EFV, TG or two mitochondrial stressors for 24h. As shown in Fig.1A, immunoblot analysis using whole-cell extracts revealed no changes in the level of total Drp1 under any of the conditions assayed, whereas the effect in the case of p-Drp1 (Ser616) was differential. Moderate mitochondrial/ER stress, such as that triggered by EFV 10 and 25μM, incremented p-Drp1 levels, an increase that was not observed with severe stress (EFV 50μM). In sharp contrast, a decrease in p-Drp1 expression was detected in cells exposed to TG, Rot or CCCP. Complex I inhibitor Rot (25μM) is a widely used pharmacological inhibitor of mitochondrial respiration, and, like EFV, inhibits complex I of the ETC, leading to a drop in $\Delta\Psi_m$ and an enhancement of mitochondrial superoxide production (Li *et al.*, 2003). The protonophore carbonyl cyanide m-chloro phenyl hydrazone CCCP (10μM) is a potent chemical uncoupler of oxidative phosphorylation which, unlike EFV or Rot, stimulates mitochondrial respiration while dissipating $\Delta\Psi_m$. ER stress was modeled with the widely utilized sesquiterpene alkaloid thapsigargin (2μM TG), a highly selective inhibitor of sarcoplasmic/endoplasmic reticulum Ca^{2+} ATPase (SERCA). Through the inhibition of SERCA, TG prevents Ca^{2+} transport into the ER lumen, which leads to its subsequent increase in the cytosol (Lytton *et al.*, 1991), thus promoting accumulation of unfolded proteins and

perturbation of intracellular Ca^{2+} homeostasis, an effect with a huge impact on mitochondrial functioning.

Regarding OPA1, an increase in the expression of its 80kDa (s-OPA1) form was recorded with all stimuli (including EFV) which occurred in a concentration-dependent-manner. Unlike this effect, the expression of 100kDa OPA1 (l-OPA1) showed no alterations with TG or Rot and the moderate concentrations of EFV (10 and 25μM), while a marked down-regulation was observed with treatment with EFV50 or CCCP. Finally, the expression of Mfn2 was severely diminished with Rot and CCCP treatment, while no significant changes were recorded with either TG or EFV. Importantly, quantitative RT-PCR analysis showed that ER-stress (TG treatment) is related to a major increase in the expression of several genes employed as markers of dynamics - *MFN1*, *MFN2*, *OPA1*, *FIS1* and *DRP1* (Fig.1B). With the exception of *DRP1*, the expression of these genes was also enhanced with EFV in a concentration-dependent fashion, whereas the classical mitochondrial stressors Rot and CCCP not only failed to trigger up-regulation *(MFN2*, *OPA1*) but actually provoked the contrary effect (*MFN1, FIS1* and *DRP1*). Considered together, these data provide evidence of a differential expression of mitochondrial fusion and fission markers under conditions of ER stress and/or different types of mitochondrial dysfunction.

Altered mitochondrial morphology was also confirmed with confocal fluorescent microscopy using the expression of the OMM protein TOM20 as a marker. Enhanced presence of "fragmented" mitochondria (small rod-like or spherical mitochondria) was observed in all treatments (Fig.2C), an effect indicative of increased fission relative to fusion. This result is in accordance with our previously published data in the same model, where mitochondria were visualized using NAO fluorescence (Polo *et al.*, 2015).

3.2. MAM – evidence for differential regulation in dual mitochondrial/ER stress

Several proteins involved in mitochondrial dynamics have been related to MAMs, including p-Drp1 and Mfn2. In this regard, we determined their specific location by studying their presence in mitochondria-enriched and cytosolic protein extracts. Firstly, we confirmed the purity of these extracts by assessment of several mitochondrial (TOM20, CIV-II and Porin) and cytosolic (LDH, Tubulin and β-actin) proteins under basal conditions and after 24h treatments (Fig.2A). We then analyzed the abundance of specific proteins related to mitochondrial dynamics. Intriguingly, cells under combined mitochondrial/ER stress tend to exhibit a slightly increased expression of p-Drp1 and Mfn2 in the cytosolic fraction although the effect was not concentration-dependent as it was not produced by the highest concentration of EFV (50μM). This quite high concentration of EFV severely damages mitochondria and the effects induced can be beyond the cellular adaptive response. On the contrary, a clear decrease is seen in cells treated with classic mitochondrial (Rot and CCCP) or ER stressors (TG) (Fig.2B). We considered that a possible explanation for the observed response was that EFV triggered *de novo* synthesis of these proteins and the time frame of 24h may not have been ample enough to have the protein inside mitochondria. However, this possibility was ruled out when analysis of the expression of p-Drp1 after prolonged treatment (48h) revealed that a differential response continued to be present (Suppl. Fig.1). Of note, the level of cell stress was crucial for this response; the highest concentration of EFV, which triggered severe mitochondrial damage, failed to produce the same effects as EFV 10 and 25μM and exerted similar actions to those of the rest of the stimuli.

The differential effect exerted by EFV in comparison with the rest of the stimuli was also confirmed by confocal microscopy experiments; there was an increase in the colocalization of p-Drp1 with the mitochondrial protein TOM20 in 10- or 25μM EFV-treated cells, which was absent with the rest of the treatments (Fig.2C).

Furthermore, we performed co-immunoprecipitation experiments to analyse the contact between specific MAM protein partners. To do this, we assessed two protein pairs: i) PTPIP51 and VAP B/C; and ii) Porin and Grp75. In both cases, the contact was enhanced in EFV-treated cells, while no increase or a significant decrease were observed with the rest of the treatments (Fig.3A,B). We also assessed the general expression of these proteins in whole cell extracts. Interestingly, the mitochondrial protein PTPIP51 displayed a major enhancement in EFV-exposed cells (Fig.3C), an effect that was not evident with the rest of the stressors. In summary, these data reveal enhancement of MAMs in cells exposed to combined ER stress/mitochondrial dysfunction.

3.3 Lon: Up-regulation and extramitochondrial location under mitochondrial/ER stress

Next, we compared the differential effects we had observed between the expression of several MAMs proteins with those exerted by another MAMs participant, Grp75 (mitochondrial HSP70), which is not directly related to mitochondrial dynamics. In this case, EFV treatment showed a similar pattern as that observed for p-Drp1 and Mfn2, with increased cytosolic content and a tendency towards a drop in mitochondrial content. In contrast, upon treatment with the other three stimuli, levels of Grp75 inside mitochondria did not diminish (Fig.4A).

Knowing that Grp75 is involved in mitochondrial proteostasis, we were interested to know whether a similar effect would be observed with another mitochondrial protein in charge of protein maintenance in this organelle; namely, the protease Lon. Also, Lon and Grp75 seem to be closely linked as Hsp60-Grp75 complex is part of the Lon interactome and the maintenance of the stability this complex by Lon´s chaperone function is crucial for cell survival (Kao *et al.*, 2015). As shown in Fig.4A, the analysis of Lon expression in cytosolic vs mitochondria-enriched fractions of EFV-treated cells revealed a very similar result to that exerted by Grp75: a decrease in the mitochondrial fraction and an increase in the extramitochondrial fraction. Once again, this was not the case with the rest of the stimuli. As mentioned previously, in

Hep3B cells, EFV leads to a concentration-dependent increase in Lon protein expression in whole cell extracts (Polo *et al*., 2015). A similar increase was also detected in HepaRG cells (Polo *et al*., 2015), a terminally differentiated hepatic cell line derived from human hepatic progenitor cells, which rules out the possibility of the effect being related to the cancerous nature of Hep3B and confirms that Hep3B are reliable cellular model for this research. In the present study, we compared this effect with that exerted by TG, Rot or CCCP and found a similar upregulation (Fig.4B). In order to assess the drug-specificity of this effect, we analyzed protein expression of Lon after treatment with a range of clinically relevant plasma concentrations of RPV, another antiretroviral drug which as EFV, belongs to the family of non-nucleoside analogues reverse transcriptase inhibitors. As shown in Fig.4C, RPV did not alter the expression of Lon. Moreover, we assessed the gene expression of *LONP1* and observed that all 4 stimuli- EFV, TG, Rot and CCCP- produced an increment of *LONP1* mRNA, although to varying extents: while the increase in the case of Rot and CCCP was modest, that induced by TG was remarkable (Fig.4D). A similar result was obtained when we treated other two cell lines, namely U-251MG, a cancerous cell line, and HUVEC, primary cell line (Fig.4D), which pointed out to a general and not cell type-specific response. Also, we observed that Lon mRNA and protein levels did not fully correlate, an effect often reported in mammalian cells, resulting from the extensive mRNA and protein content regulation at different levels, and particularly observed in cells subjected to protein misfolding stress (Cheng *et al.*, 2016).

3.4 The mechanisms involved in Lon up-regulation: evidence for the significance of dual mitochondrial/ER stress

In order to assess the regulation of Lon upregulation, we transiently silenced the transcription factor *CHOP* and examined the protein level of Lon in whole cell extracts by WB. We confirmed the expected increase in CHOP by EFV, Rot and TG (in accordance with our

previously published work) and found out that siCHOP cells exhibited similar Lon levels as siControls, which would suggest that this transcription factor is not involved in the regulation of Lon expression (Suppl. Fig.2). Another transcription factor that we speculated could be involved in *LONP1* upregulation in our model is nuclear factor- kappa B (NF-*k*B). In order to test this possibility, we performed ChiP assay, a technique used for probing protein-DNA interactions within the natural chromatin context of the cell. These experiments revealed that EFV treatment concentration-dependently increased the contact between NF-*k*B and the promoter of *LONP1* (Fig.4E). While *LONP1* expression is regulated by NF-κB upon EFV treatment, we haven´t observed such a transcriptional regulation in TG-treated cells, a finding which may point to an alternative transcription factor involved under classical ER stress (TG) probably signalled by one or several of the UPR signal transduction arms. One possibility is NRF2 which is regulated via the PERK-ATF4 branch and is among the major transcriptional regulators of *LONP1*. Moreover, the specificity of Lon expression was evidenced by the fact that neither of the treatments altered the expression of ClpX, another ATP-dependent MM protease (Fig.4F).

To further delve in the mechanism by which Lon is up-regulated, we assessed the activation of PERK, one of the master regulators of the UPR in mammalian cells. During conditions of ER stress, PERK undergoes autophosphorylation of its kinase domain which increases its activity. 24h-treatment with EFV led to a slight increase in the presence of p-PERK studied by WB (Fig.5A) which was visible with EFV10 and EFV25 but not EFV50. A similar increasing effect was observed with CCCP while TG led to a significant decrease in the protein content of p-PERK. However, pharmacological inhibition of PERK phosphorylation achieved with the selective inhibitor GSK2656157 had only a minor effect on EFV-induced Lon protein expression as observed with EFV10 and EFV25 (Fig.5A). The lack of a major regulatory effect

of p-PERK was confirmed by RT-PCR analysis of *LONP1* in cells exposed to EFV in the presence of p-PERK inhibitor (Fig.5B).

It is widely known that *LONP1´*s transcription is promoted in conditions of oxidative stress. Given that EFV increments mitochondrial superoxide production in this model (Apostolova *et al.*, 2010, Polo *et al.*, 2015), we sought to explore the participation of oxidative species in Lon up-regulation. For this, 24h-treatments were performed in the presence of MnTMPyP, a metalloporphyrin-based superoxide dismutase/catalase mimetic. Both protein (Fig.5A) and mRNA expression (Fig.5B) analysis revealed that oxygen radicals participate in EFV-induced Lon up-regulation.

3.5 Implications of incremented Lon: protection against oxidative stress

Having observed that Lon was up-regulated in cells exposed to EFV, we wished to assess the role of this increase in the cellular effect of the drug. To this end, EFV treatment was performed in cells where *LONP1* was transiently silenced (Fig.6A) and compared to that performed in siControl cells. As mentioned previously, 24h-exposure to EFV compromises cell viability and alters mitochondrial function (increased mitochondrial mass, enhanced ROS generation and diminished $\Delta\Psi_m$). As depicted in Fig.6B, while Lon does not seem to influence the effect of EFV on cell viability (assessed as number of nuclei), mitochondrial mass (NAO fluorescence) and $\Delta\Psi_m$ (TMRM fluorescence), we observed that siLONP1 cells displayed a higher level of EFV-induced mitochondrial superoxide production (MitoSox fluorescence).

3.6 Lon is associated with the ER/MAMs in dual mitochondrial/ER stress

Having observed that Lon presence in the extramitochondrial fraction increases following EFV treatment, we sought to analyze its intracellular location. To do this, we performed double-staining immunocytochemistry experiments by confocal fluorescence microscopy using the chaperone Calnexin as a protein marker for ER. Colocalization analysis revealed an increased overlapping between the Lon signal and the ER in cells exposed to EFV, while no changes

were observed with the rest of the stimuli (Fig.7A). In view of this finding and the results we obtained previously by immunoblot experiments (Fig.4A), we decided to use the same approach of confocal microscopy to assess mitochondrial Lon localization by studying its association with the mitochondrial matrix signal coming from the fluorochrome MitoView which accumulates in the matrix of polarized mitochondria. As depicted in Fig.7B, EFV leads to a decrease in Lon´s presence in the mitochondrial matrix.

Calnexin itself is considered a MAMs protein, which made us speculate about Lon´s location in MAMs. In order to assess this possibility, we next obtained subcellular fractions (crude mitochondria, ER, cytosol and MAMs) of cells treated with EFV, TG or CCCP and explored the presence of several protein markers. The grade of purity of the samples was assessed by studying the abundance of specific proteins in the untreated cell extracts (Fig.8A) and the obtained results were similar to those reported elsewhere (Wieckowski *et al.*, 2009). While Porin, a MAM protein was observed both in crude mitochondria and MAM fractions, MAMs lacked Cytochrome *c*, a MM protein, as expected. The mitochondrial protein and reported MAM component FACL4 was highly abundant in crude mitochondria and MAMs, but was also detected in the ER and the cytosol. Virtually all Lon was located in the mitochondria, as anticipated. Subsequently, we compared the presence of two mitochondrial proteins recognized as MAM members (Grp75 and PTPIP51) under different pharmacological treatments and contrasted this with the expression of Lon (Fig.8B). PTPIP51 was detected only in the crude mitochondria fraction, while EFV induced a major increment in its expression, in accordance with the experiments using whole cell extracts (Fig3C). Grp75 was present in all four fractions, and EFV increased its presence notably in the cytosol, ER and MAMs. Interestingly, the pattern of Lon expression was very similar to that of Grp75, pointing to the possibility that Lon is itself a MAM protein whose presence in MAM is greatly incremented under combined ER/mitochondrial stress. We also assessed the levels of Calnexin, an ER-resident chaperone

and Ca-binding protein, and a MAMs component itself, in the same extracts (Suppl. Fig.3). The cytosolic samples obtained after treatment with the different stimuli (EFV, TG and CCCP) displayed no changes in the content of Calnexin in comparison to the control, while the presence of the protein in the RE fraction in all three cases decreased. Interestingly, this was paralleled by an increase in the presence of Calnexin in the MAMs fraction which was modest in the case of EFV and dramatic in the case of TG. Such evident difference in the levels of Calnexin in the MAMs between TG (classical ER stressor) and EFV point again to the specificity of the action of EFV.

4. Discussion

Regulation of mitochondrial dynamics/morphology is paramount for proper mitochondrial functioning (Vannuvel *et al.*, 2013). While mitochondrial fusion facilitates the exchange of vital metabolites and mtDNA between different mitochondria to ensure their functional maintenance (Nakada *et al.*, 2009), mitochondrial fission is required to ensure biogenesis, to respond to changes in local energy demands and to separate/eliminate damaged or old mitochondria through a selective autophagic process called mitophagy. Mitochondrial fusion and fission are tightly controlled processes that require several highly evolutionary conserved GTPases: mitofusins, anchored in the OMM (Santel and Fuller, 2001); OPA1, located in the IMM (Smirnova *et al.*, 1998); and Drp1 (Otera and Mihara, 2011). During the import of OPA1 into the MM, the N-terminal matrix-targeting signal (MTS) is cleaved by mitochondrial processing peptidase (MPP) to form the mature OPA1 isoform (L-isoform) (Ishihara *et al.*, 2006), which undergoes further processing events at two distinct sites - S1 and S2 - generating shorter isoforms. L-isoform has a mitochondrial fusion-stimulating activity, a feature that is lost following proteolytic cleavage into the S-isoform (Ishihara *et al.*, 2006). There is evidence that mitochondrial dysfunction, characterized by low mitochondrial ATP production and $\Delta\Psi_m$ dissipation, is associated with loss of the long isoform (Vannuvel *et al.*, 2013). This is in line

with other results of the present work, which demonstrate that mitochondrial/ER stressors reduce the l-OPA1/s-OPA1 ratio, which is particularly evident under the conditions that cause massive $\Delta\Psi_m$ loss. The master regulator of mitochondrial division in most eukaryotic organisms, Drp1, is mostly cytosolic, with only approximately 3% associated to the OMM (Smirnova *et al.*, 2001). In order to promote fusion, Drp1 is recruited to mitochondria, where it oligomerizes around the mitochondrion, thus constricting it. Many studies have failed to report an increase in fission through the alteration of protein levels of Drp1, which is in line with the results shown here. On the contrary, it seems that post-translational modifications target Drp1 to mitochondria and enable it to mediate fission. One such regulation is phosphorylation at Ser616, which occurs through Cdk1/cyclin B (Taguchi *et al.*, 2007) and triggers mitotic Drp1-dependent mitochondrial fission. Since this modification does not directly affect GTPase activity, the increase in fission may be mediated by alterations in Drp1 interactions with other proteins. In the present model, the dual effect of ER stress/mitochondrial dysfunction led to an increase in Drp1-p expression and its co-localization with mitochondria, an effect that was not achieved with the rest of the stimuli. In summary, it is crucial to understand that different stimuli that produce ER-stress and/or different types of mitochondrial dysfunction regulate markers of mitochondrial dynamics in a differential way.

Abundant evidence demonstrates that mitochondria function in close collaboration with the ER, but precisely how this is affected by distinct pathophysiological conditions remains to be determined. On examining the role of Lon we have found that its content in the mitochondrion is depleted upon dual ER stress/mitochondrial dysfunction, while its extramitochondrial presence - in both the ER and MAMs - is increased. This, however, is not the case when cells are exposed to classical mitotoxic stimuli such as Rot or CCCP, which underlines, once more, the importance of the role of ER-stress in this phenomenon. A considerable body of evidence shows that Lon is upregulated during ER-stress and that this occurs through the PERK-ATF4

pathway (Hori, *et al. 2002*; Rainbolt *et al.*, 2013) or with the participation of the transcription factor CHOP (CCAAT-enhancer-binding protein homologous protein) (Han *et al.*, 2013). In the present model, PERK phosphorylation seems to be only partially involved in Lon up-regulation while CHOP does not seem to participate, and *LONP1* expression is controlled by NF-*k*B, as suggested by other studies (Pinti *et al.*, 2011). The uncoupler CCCP can induce ER stress as seen in SH-SY5Y exposed to 10μM CCCP for 24h (Bouman et al., 2010), an experimental setting similar to ours. Although we have not addressed whether this occurs specifically in our model, it is evident that in the majority of the parameters EFV and CCCP do not produce the same effect. In this regard, while EFV (25μM) and CCCP (10μM) lead to similar drop in $\Delta\Psi_m$ after 24h-treatment (Polo M et al., 2015), the extent of up-regulation of *LONP1* induced by the two stressors differs greatly.

Although the regulatory mechanisms governing Lon expression are still somewhat elusive, there is a growing body of evidence that pinpoints Lon as a human stress protein whose levels increase after exposure to multiple independent stressors including heat shock, hypoxia, serum starvation, and oxidative stress (Ngo *et al.*, 2013). In this regard, we have proven the participation of oxidants in Lon´s up-regulation and the protective role of Lon regarding oxidative stress in our model.

In light of our results, it is tempting to speculate on Lon´s location during specific cellular insults. Moreover, Lon is regarded as MM protease hence its up-regulation upon the mentioned stress stimuli would be assumed to enhance its canonical mitochondrial function. With this, studies that report stress-induced Lon up-regulation do not assess its sub-cellular localization (Hori *et al.*, 2002).

The pattern of Lon and Grp75 expression under TG and EFV treatment studied by WB show both similarities and differences. However, the specificity of the WB analysis of mitochondria-enriched vs cytosolic extracts is not sufficient and extracts representing extramitochondrial protein fractions may include MAM proteins (specifically outer mitochondrial membrane-associated), which is why we performed a more accurate analysis of subcellular fractionation. This experiment clearly showed an increase of both Grp75 and Lon induced by TG and EFV in MAMs. Regarding ER fraction, TG does not increment Lon´s level, which is in line with the result obtained by confocal microscopy that revealed no increased association between Lon and calnexin, used as an ER-marker, in TG-treated cells. Also, the present study reflects that there are several differences between the effect of TG and that of EFV on Lon regulation, however whether this would be the case with other pharmacological ER stressors remains to be elucidated.

Our study leads to several conclusions: firstly, mitochondrial dynamics and mitochondria/ER contact are differentially regulated upon different types of mitochondrial and ER-stress; secondly, Lon is transcriptionally upregulated under these conditions - this effect is not cell-type specific as it occurs in different cell types and is not related to the drug family of EFV as it was not recorded with RPV, member of the same family of antiretroviral drugs, which does not affect neither mitochondrial nor ER function in Hep3B cells (Blas-Garcia *et al.*, 2014); and, thirdly, and most importantly, Lon is involved in the interorganellar crosstalk between the ER and mitochondria as a MAM component itself. What exactly is its putative role in the MAMs is unknown and remains to be explored. The mechanisms involved in MAMs assembly are still not understood which limits our knowledge of how signal transduction might impact ER–mitochondria associations. It is plausible, however, that changes in physiological demands of the cell (e.g., requirements for increased mitochondrial ATP, altered Ca flux or altered lipid production) might signal to induce morphological changes in ER–mitochondria contact sites

that could facilitate such demands. In this work, we have used Grp75 as a reference mitochondrial MAM´s component due to its similarities with Lon. Both are mitochondrial matrix proteins which even physically interact (Kao *et al.*, 2015), they are involved in the proteostasis of this organelle, and both are induced by ER-stress (Hori *et al.*, 2002). Whether the mechanism by which Lon participates in the MAMs is similar to that of Grp75 is yet to be studied. Lon is a matrix protein, however it can be recruited to the IMM and interact with prohibitins (Bulteau and Bayot, 2011).

In control cells and upon ectopic expression of the WT protein, Lon can be found in the mitochondrial matrix (Hori et al., 2002). We provide evidence of its alternative location in stressed cells. This finding is in line with a recent proteomics study which identified Lon as a mitochondrial antiviral-signaling protein **(**MAVS)-interacting protein during RNA virus infection *in vitro* (Horner *et al.*, 2015). MAVS, an OMM protein and itself considered a MAMs component, is recognized as a crucial participant in the innate immune response to RNA virus infection in mammalian cells. The fact that Lon regulation occurs in the presence of an antiretroviral drug, as shown by our results, significantly bolsters the findings of said study and open a new and very promising route for research. The presence of Lon in MAMs could also be cell type-specific - Lon was identified in an in-depth proteomic analysis of MAMS obtained from mouse brain samples under basal conditions but not from liver (Poston CN *et al.*, 2013). We believe that the findings presented here contribute in a considerable way to the growing knowledge regarding mitochondria-ER inter-regulations. Indeed, we hope they are a starting point for a more comprehensive understating of the role of Lon under complex stressful conditions. The findings shown here are potentially clinically relevant due to the fact that the effects were observed with Efavirenz, one of the most widely used antiretroviral drugs.

5. Acknowledgments

The authors thank Brian Normanly for his English language editing and Dr Ricardo Flores Pedauyé (Research Professor, CSIC) for assistance with the cellular subfractionation experiments which were performed at Instituto de Biología Molecular y Celular de Plantas (UPV-CSIC), Valencia, Spain.

Ca^{2+} - http://www.guidetopharmacology.org/GRAC/LigandDisplayForward?ligandId=707

6. Funding

This work was supported by the Instituto de Salud Carlos III, Ministerio de Economía y Competitividad (research grant PI14/00312 and CIBER CB06/04/0071, postgraduate fellowship FI12/00198 to FA and "Juan de la Cierva" postdoctoral contract JCI-2012–15124 to AB-G); the Conselleria d'Educació, Formació i Ocupació, Generalitat Valenciana (research grants PROMETEOII/2014/035, ACOMP/2013/236 and GVA/2014/118, and postgraduate fellowship ACIF/2013/136 to MP) and Ministerio de Educación, Cultura y Deporte (postgraduate fellowship FPU13/00151 to AM-R). ABM is the recipient of Postgraduate Trainee Research Grant from Fundación Juan Esplugues.

7. Conflicts of interest

JVE has received funds for speaking at symposia organized by Abbvie Farmacéutica S.L.U., Astra Zeneca and Gilead Sciences. All other authors: none to declare.

8. References

Apostolova N, Gomez-Sucerquia LJ, Alegre F, Funes HA, Victor VM, Barrachina MD, et al (2013). ER stress in human hepatic cells treated with Efavirenz: mitochondria again. J Hepatol 59(4), 780-789.

Apostolova N, Gomez-Sucerquia LJ, Moran A, Alvarez A, Blas-Garcia A, Esplugues JV (2010). Enhanced oxidative stress and increased mitochondrial mass during efavirenz-induced apoptosis in human hepatic cells. Br J Pharmacol 160(8), 2069-2084.

Blas-García A, Polo M, Alegre F, Funes HA, Martínez E, Apostolova N, et al (2014). Lack of mitochondrial toxicity of darunavir, raltegravir and rilpivirine in neurons and hepatocytes: a comparison with efavirenz. J Antimicrob Chemother 69(11): 2995-3000.

Bota DA, Davies KJ (2002). Lon protease preferentially degrades oxidized mitochondrial aconitase by an ATP-stimulated mechanism. Nat Cell Biol 4(9): 674-680.

Bouman L, Schlierf A, Lutz AK, Shan J, Deinlein A, Kast J, et al (2011). Parkin is transcriptionally regulated by ATF4: evidence for an interconnection between mitochondrial stress and ER stress. Cell Death Differ 18(5): 769-82.

Bui M, Gilady SY, Fitzsimmons RE, Benson MD, Lynes EM, Gesson K, et al (2010). Rab32 modulates apoptosis onset and mitochondria-associated membrane (MAM) properties. J Biol Chem 285(41), 31590-31602.

Bulteau AL, Bayot A (2011). Mitochondrial proteases and cancer. Biochim Biophys Acta. 1807(6), 595-601.

Burger D, van der Heiden I, la Porte C, van der Ende M, Groeneveld P, Richter C, et al (2006). Interpatient variability in the pharmacokinetics of the HIV non-nucleoside reverse transcriptase inhibitor efavirenz: the effect of gender, race, and *CYP2B6* polymorphism. Br J Clin Pharmacol 61(2): 148–154.

Carr DF, la Porte CJ, Pirmohamed M, Owen A, Cortes CP (2010). Haplotype structure of CYP2B6 and association with plasma efavirenz concentrations in a Chilean HIV cohort. J Antimicrob Chemother 65(9): 1889-1893.

Cheng Z, Teo G, Krueger S, Rock TM, Koh HW, Choi H, Vogel C (2016). Differential dynamics of the mammalian mRNA and protein expression response to misfolding stress. Mol Syst Biol 12(1), 855.

Curtis MJ, Bond RA, Spina D, Ahluwalia A, Alexander SPA, Giembycz MA, et al. (2015). Experimental design and analysis and their reporting: new guidance for publication in BJP. Br J Pharmacol 172: 3461–3471.

de Brito OM, Scorrano L (2008). Mitofusin 2 tethers endoplasmic reticulum to mitochondria. Nature 456(7222), 605-610.

Friedman JR, Lackner LL, West M, DiBenedetto JR, Nunnari J, Voeltz GK (2011). ER tubules mark sites of mitochondrial division. Science 334(6054), 358-362.

Fukuda R, Zhang H, Kim JW, Shimoda L, Dang CV, Semenza GL (2007). HIF-1 regulates cytochrome oxidase subunits to optimize efficiency of respiration in hypoxic cells. Cell 129(1), 111-122.

Funes HA, Apostolova N, Alegre F, Blas-Garcia A, Alvarez A, Marti-Cabrera M, et al (2014). Neuronal bioenergetics and acute mitochondrial dysfunction: a clue to understanding the central nervous system side effects of efavirenz. J Infect Dis 210(9): 1385-1395.

Giorgi C, De Stefani D, Bononi A, Rizzuto R, Pinton P (2009). Structural and functional link between the mitochondrial network and the endoplasmic reticulum. Int. J. Biochem. Cell Biol 41(10), 1817-1827.

Gounden V, van Niekerk C, Snyman T, George JA (2010). Presence of the CYP2B6 516G> T polymorphism, increased plasma Efavirenz concentrations and early neuropsychiatric side effects in South African HIV-infected patients. AIDS Res Ther 7: 32.

Han J, Back SH, Hur J, Lin YH, Gildersleeve R, Shan J, et al. (2013). ER-stress-induced transcriptional regulation increases protein synthesis leading to cell death. Nat. Cell Biol 15(5), 481-490.

Hori O, Ichinoda F, Tamatani T, Yamaguchi A, Sato N, Ozawa K, et al. (2002). Transmission of cell stress from endoplasmic reticulum to mitochondria: enhanced expression of Lon protease. J Cell Biol 157(7), 1151-1160.

Horner SM, Wilkins C, Badil S, Iskarpatyoti J, Gale M Jr (2015). Proteomic analysis of mitochondrial-associated ER membranes (MAM) during RNA virus infection reveals dynamic changes in protein and organelle trafficking. PLoS One 10(3), e0117963.

Ishihara N, Fujita Y, Oka T, Mihara K (2006). Regulation of mitochondrial morphology through proteolytic cleavage of OPA1. EMBO J 25(13), 2966-2977.

Kao TY, Chiu YC, Fang WC, Cheng CW, Kuo CY, Juan HF, et al (2015). Mitochondrial Lon regulates apoptosis through the association with Hsp60-mtHsp70 complex. Cell Death Dis 6:e1642.

Li N, Ragheb K, Lawler G, Sturgis J, Rajwa B, Melendez JA, et al. (2003). Mitochondrial complex I inhibitor rotenone induces apoptosis through enhancing mitochondrial reactive oxygen species production. J Biol Chem 278(10), 8516-8525.

Lin J, Schyschka L, Mühl-Benninghaus R, Neumann J, Hao L, Nussler N, et al (2012). Comparative analysis of phase I and II enzyme activities in 5 hepatic cell lines identifies Huh-7 and HCC-T cells with the highest potential to study drug metabolism. Arch Toxicol 86(1), 87-95.

Lodish H, Berk A, Zipursky SL, Matsudaira P, Baltimore D, Darnell J (2000). Molecular Cell Biology. 4th edition. New York: W. H. Freeman.

Lytton J, Westlin M, Hanley MR (1991). Thapsigargin inhibits the sarcoplasmic or endoplasmic reticulum Ca-ATPase family of calcium pumps. J Biol Chem 266(26), 17067-17071.

Matsushima Y, Goto Y, Kaguni LS (2010). Mitochondrial Lon protease regulates mitochondrial DNA copy number and transcription by selective degradation of mitochondrial transcription factor A (TFAM). Proc Natl Acad Sci U S A 107(43), 18410-18415.

Nakada K, Sato A, Hayashi J (2009). Mitochondrial functional complementation in mitochondrial DNA-based diseases. Int. J. Biochem. Cell Biol 41(10), 1907-1913.

Ngo JK, Pomatto LC, Davies KJ (2013). Upregulation of the mitochondrial Lon Protease allows adaptation to acute oxidative stress but dysregulation is associated with chronic stress, disease, and aging. Redox Biol 1, 258-264.

Otera H, Mihara K (2011). Discovery of the membrane receptor for mitochondrial fission GTPase Drp1. Small GTPases 2(3), 167-172.

Polo M, Alegre F, Funes HA, Blas-Garcia A, Victor VM, Esplugues JV, et al. (2015). Br J Pharmacol 172(7), 1713-1727.

Poston CN, Krishnan SC, Bazemore-Walker CR (2013). In-depth proteomic analysis of mammalian mitochondria-associated membranes (MAM). J Proteomics 79, 219-230.

Rainbolt TK, Saunders JM, Wiseman RL (2014). Stress-responsive regulation of mitochondria through the ER unfolded protein response. Trends Endocrinol Metab 25(10), 528-537.

Santel A, Fuller MT (2001). Control of mitochondrial morphology by a human mitofusin. J Cell Sci 114(Pt 5), 867-874.

Smirnova E, Griparic L, Shurland DL, van der Bliek AM. (2001). Dynamin-related protein Drp1 is required for mitochondrial division in mammalian cells. Mol Biol Cell 12(8), 2245–2256.

Smirnova E, Shurland DL, Ryazantsev SN, Van Der Bliek AM (1998). A human dynamin-related protein controls the distribution of mitochondria. J Cell Biol. 143, 351–358.

Southan C, Sharman JL, Benson HE, Faccenda E, Pawson AJ, Alexander SP *et al.* (2016). The IUPHAR/BPS Guide to PHARMACOLOGY in 2016: towards curated quantitative interactions between 1300 protein targets and 6000 ligands. Nucl Acids Res 44: D1054-1068.

Szabadkai G, Bianchi K, Várnai P, De Stefani D, Wieckowski MR, Cavagna D, et al. (2006). Chaperone-mediated coupling of endoplasmic reticulum and mitochondrial Ca2+ channels. J Cell Biol 175(6), 901-911.

Pinti M, Gibellini L, De Biasi S, Nasi M, Roat E, O'Connor JE, et al. (2011). Functional characterization of the promoter of the human Lon protease gene. Mitochondrion 11(1), 200-206.

Taguchi N, Ishihara N, Jofuku A, Oka T, Mihara K. (2007). Mitotic phosphorylation of dynamin-related GTPase Drp1 participates in mitochondrial fission. J Biol Chem 282(15), 11521-11529.

Vance JE (1990). Phospholipid synthesis in a membrane fraction associated with mitochondria. J Biol Chem 265(13), 7248-7256.

Vannuvel K, Renard P, Raes M, Arnould T (2013). Functional and morphological impact of ER stress on mitochondria. J Cell Physiol 228(9), 1802-1818.

Wieckowski MR, Giorgi C, Lebiedzinska M, Duszynski J, Pinton P (2009). Isolation of mitochondria-associated membranes and mitochondria from animal tissues and cells. Nat Protoc 4(11), 1582-1590.

Zhu XH, Wang CH, Tong YW (2007). Growing tissue-like constructs with Hep3B/HepG2 liver cells on PHBV microspheres of different sizes. J Biomed Mater Res B Appl Biomater 82(1),7-16.

Fig. 1

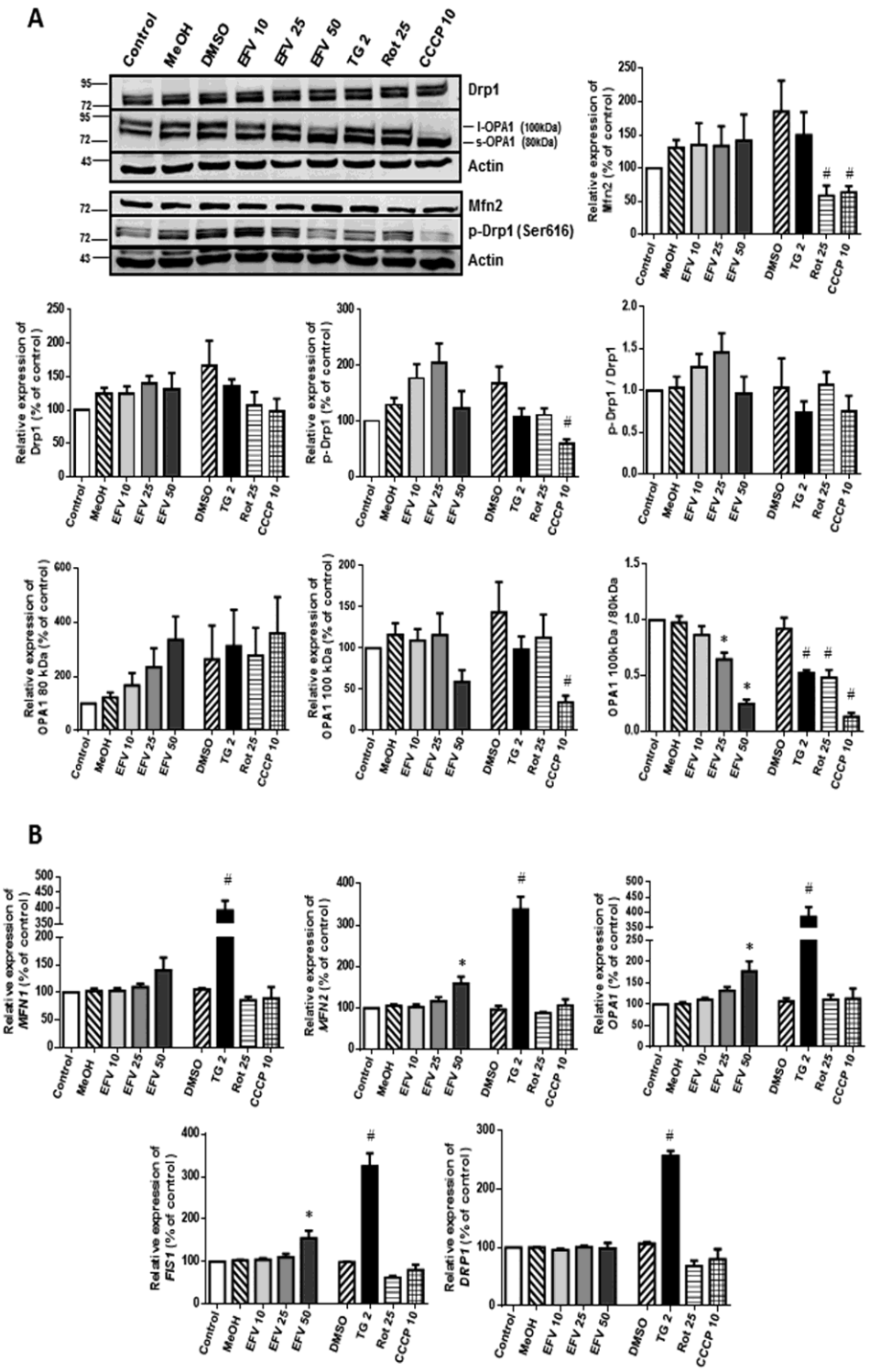

Fig.1 Expression of main molecular mediators of mitochondrial dynamics. Cells were treated for 24h with increasing concentrations of efavirenz (EFV), vehicles (MeOH or DMSO), thapsigargin (TG) 2µM, rotenone (Rot) 25µM or CCCP 10µM. (**A**) Immunoblot analysis showing representative WB image and histograms expressing quantification of the main

regulators of mitochondrial fusion and fission. Data (mean±SEM, n=6 for OPA1; n=5 for Drp1 y p-Drp1; n=8 for Mfn2) are expressed as % of control, the negative control (untreated cells) being considered 100%. (**B**) Gene expression analyzed by quantitative RT-PCR. Data (mean±SEM, n=5) are expressed as mRNA content in relation to that of control (untreated cells, considered 100%) after normalization with the expression of the housekeeping gene *ACTB* (β-actin). Statistical analysis was performed by One-way ANOVA ($^{*}P<0.05$ for EFV vs MeOH and $^{\#}P < 0.05$ for TG, Rot or CCCP vs DMSO).

Fig. 2

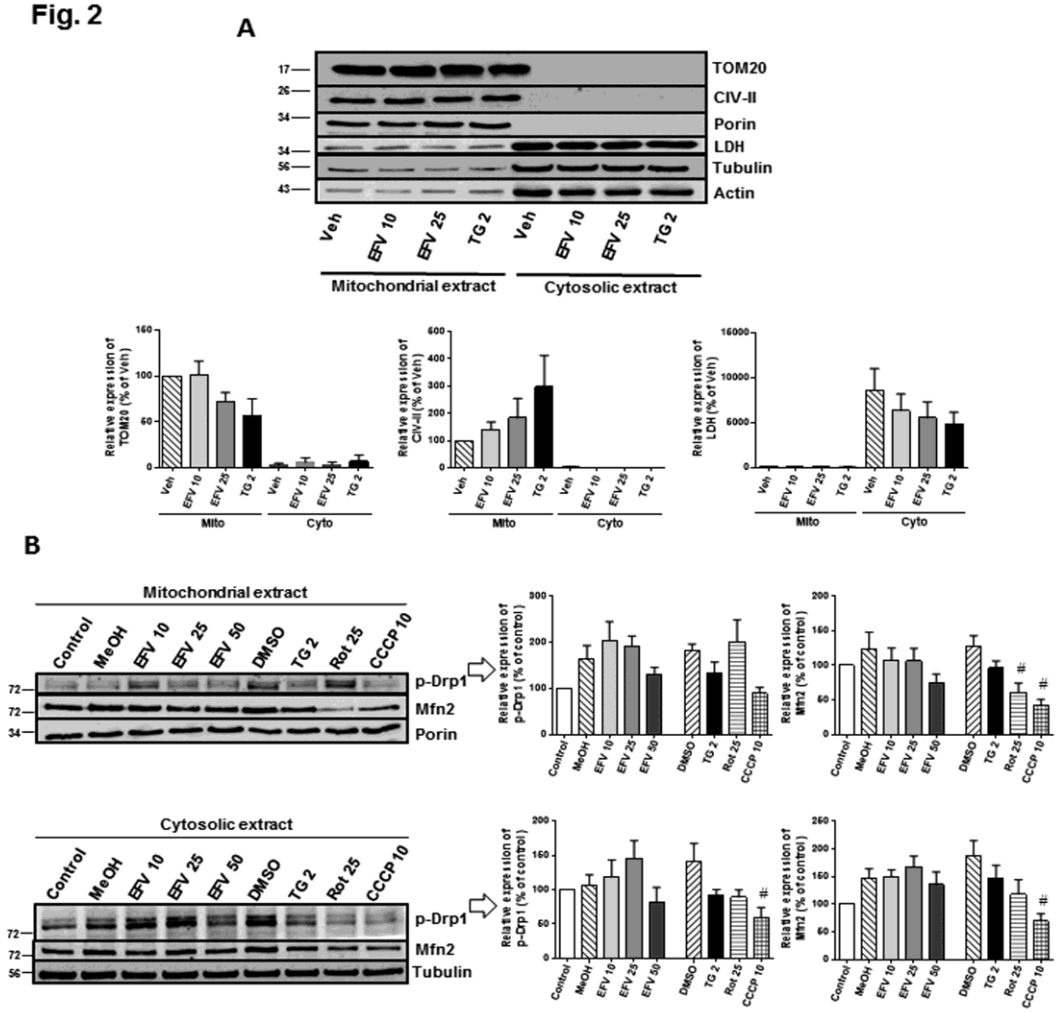

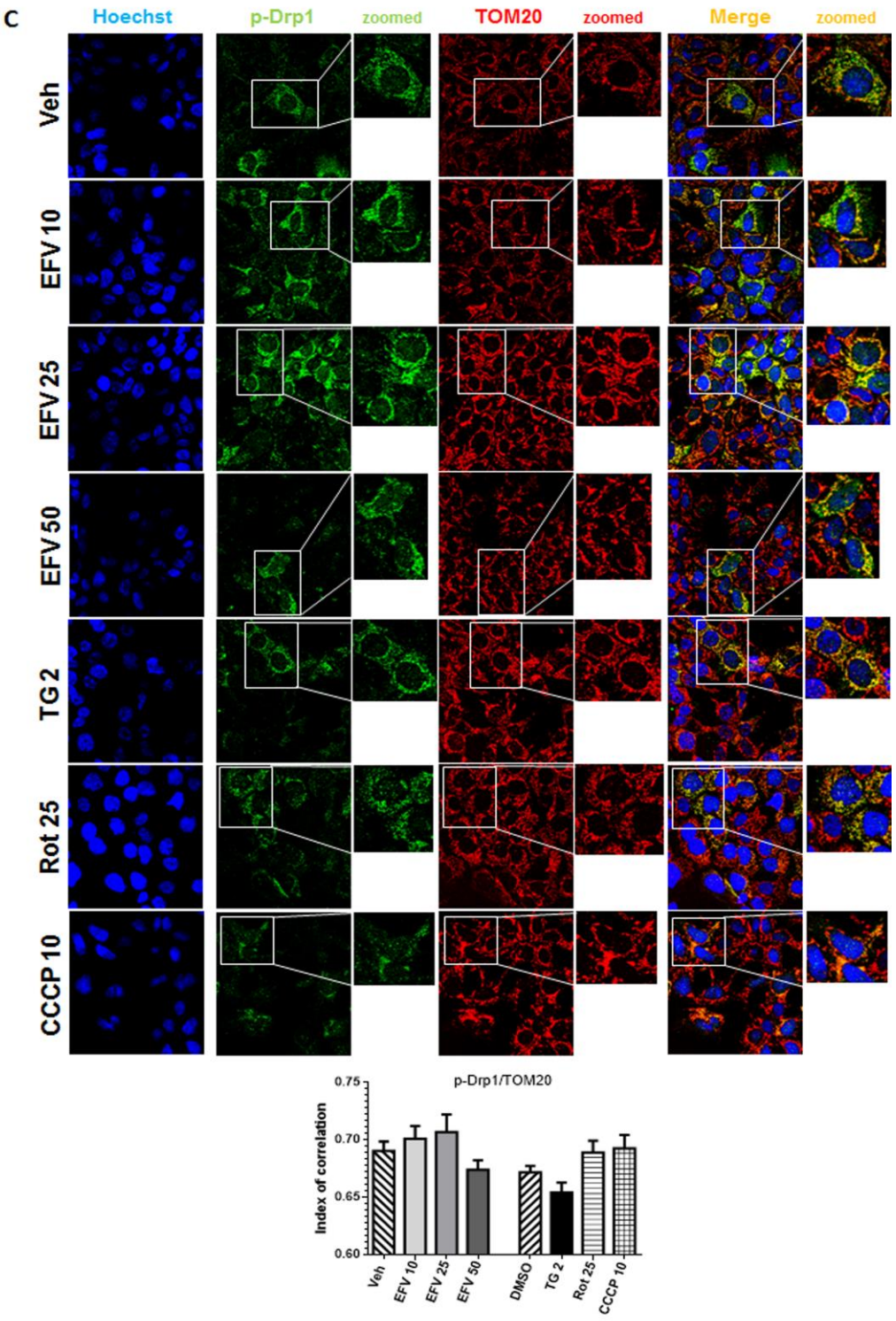

Fig.2. p-Drp1 and Mfn2 sub-cellular protein expression. (**A**) Analysis of the purity of mitochondria-enriched and cytosolic protein extracts. Representative WB image and histograms expressing quantification of several mitochondrial (TOM20, CIV-II and Porin) and cytosolic (LDH, Tubulin and β-actin) proteins after 24h of treatment. Data (mean±SEM, n=6) are expressed as % of control in the mitochondrial fraction, untreated cells considered 100%.

(**B**) WB analysis of p-Drp1 and Mfn2 in mitochondrial and cytosolic extracts in cells treated for 24h with increasing concentrations of efavirenz (EVF), vehicles (MeOH and DMSO), thapsigargin (TG) 2µM, rotenone (Rot) 25µM or CCCP 10µM. A representative image and histograms of the data quantification are shown. Data (mean±SEM, n=6) are expressed as % of control, untreated cells considered 100%. (**C**) Translocation of p-Drp1 to mitochondria. Cells were treated for 24h with increasing concentrations of efavirenz (EFV), vehicle, thapsigargin (TG) 2µM, rotenone (Rot) 25µM or CCCP 10µM. Representative confocal microscopy images (63x) of cells labeled with Hoechst 33342 (nuclei), anti-p-Drp1 (Ser616) and anti-TOM20 (mitochondria). Histogram showing the index of correlation between p-Drp1 and mitochondria (mean±SEM, n=5). Statistical analysis was performed by One-way ANOVA ($^{\#}P < 0.05$ for Rot or CCCP vs DMSO).

Fig. 3

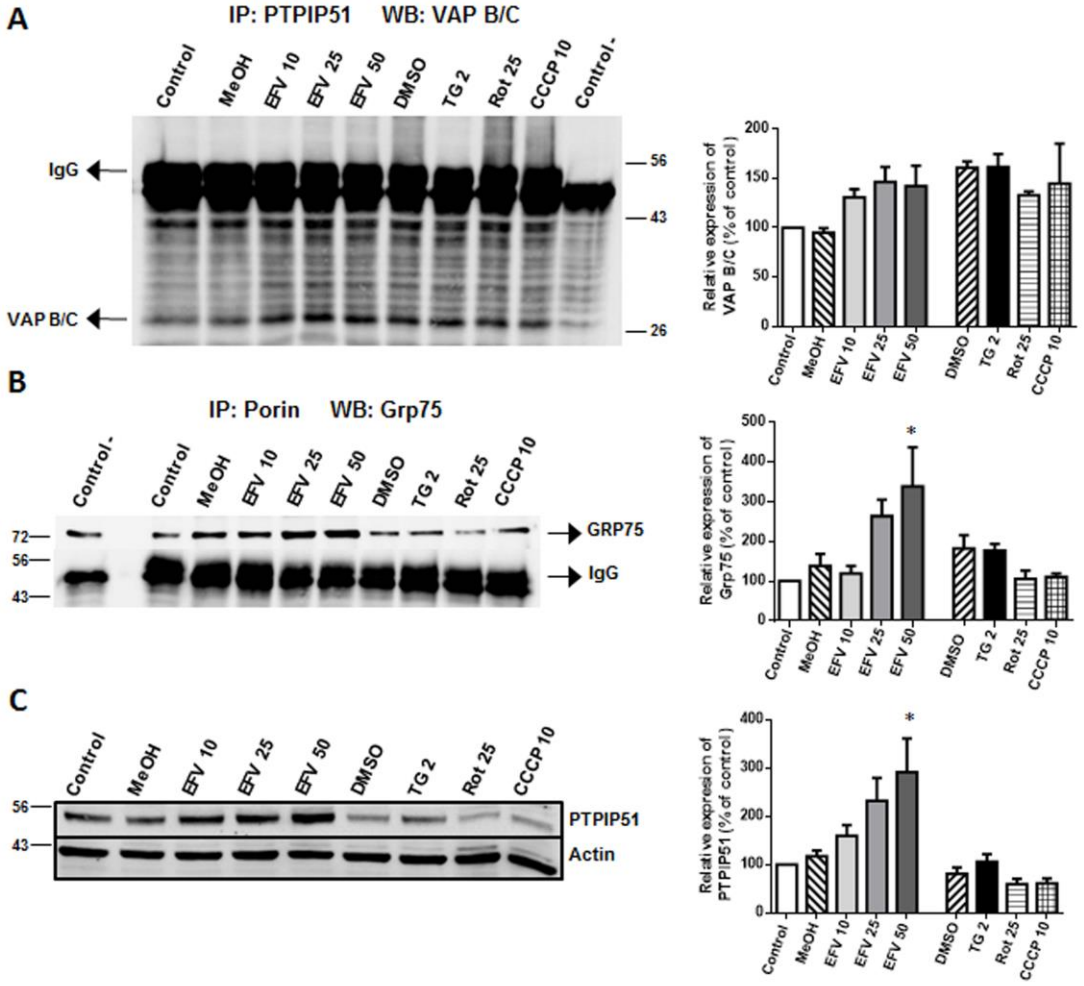

Fig.3. Study of Mitochondria-Associated ER membranes (MAMs). Cells were treated for 24h with increasing concentrations of efavirenz (EVF), vehicles (MeOH or DMSO), thapsigargin (TG) 2µM, rotenone (Rot) 25µM or CCCP 10µM. (**A, B**) Analysis of contact between specific MAM protein partners by co-immunoprecipitation using protein A sepharose beads. Representative WB images and histograms expressing quantification of (**A**) VAP B/C after immunoprecipitation of PTPIP51 and (**B**) Grp75 after immunoprecipitation of Porin. A negative control (without primary antibody) was used as control of the immunoprecipitation. (**C**) WB analysis of PTPIP51 expression in whole cell extracts. Data (mean±SEM, n=5) are expressed as % of control (untreated cells, considered 100%). Statistical analysis was performed by One-way ANOVA ($^{*}P<0.05$ for EFV vs MeOH).

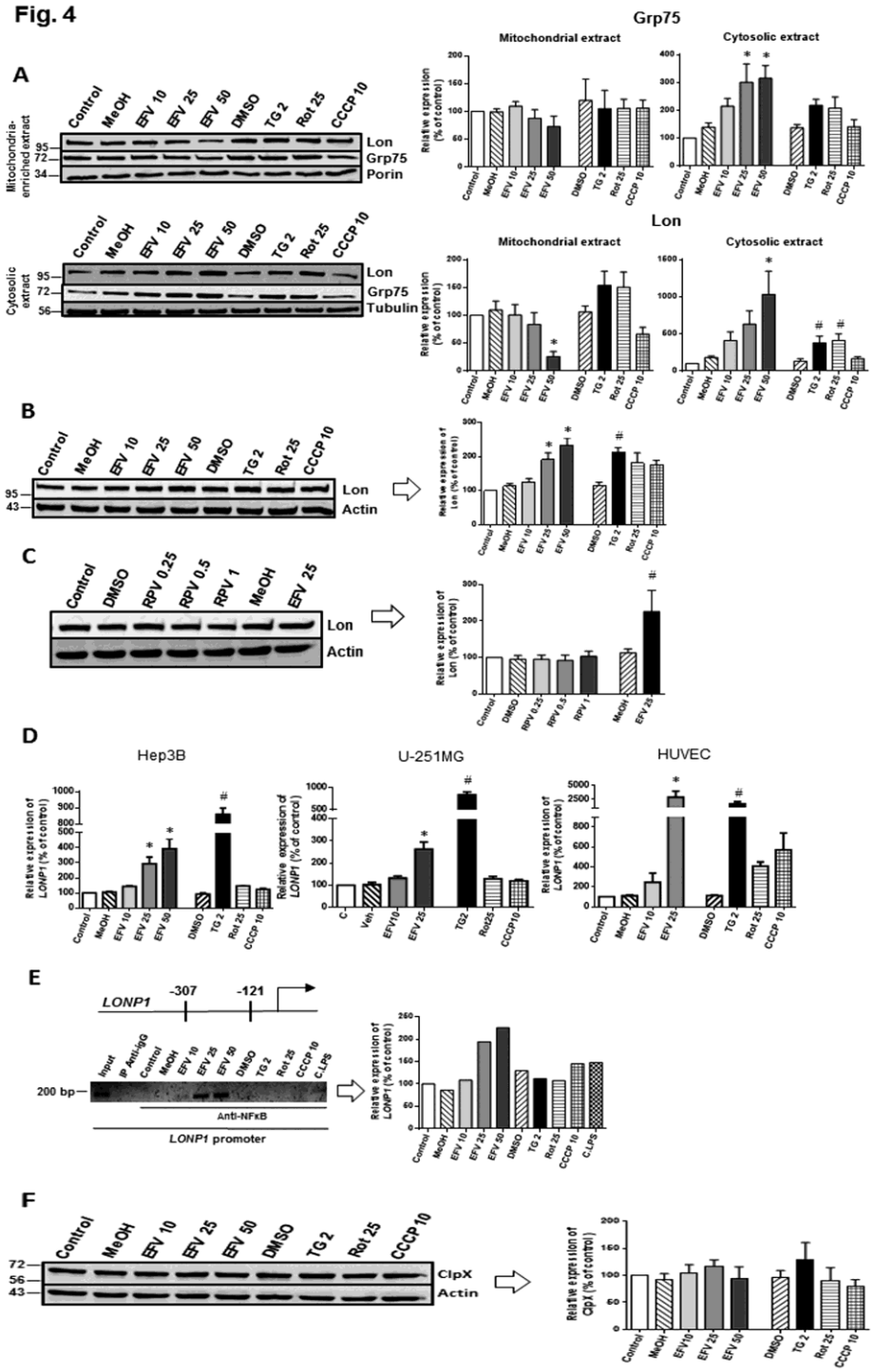

Fig.4. Analysis of Lon´s expression. Cells were treated for 24h with increasing concentrations of efavirenz (EVF), vehicles (MeOH or DMSO), thapsigargin (TG) 2µM, rotenone (Rot) 25µM or CCCP 10µM except for (C). (**A**) Representative WB images and histograms expressing quantification of Grp75 and Lon in mitochondria-enriched and cytosolic protein extracts (mean±SEM, n=6). (**B**) WB analysis of Lon expression in whole cell protein extracts

(mean±SEM, n=6). (**C**) WB analysis of Lon expression in whole cell protein extracts obtained from Hep3B cells after 24h treatment with rilpivirine (RPV), (mean±SEM, n =5). (**D**) Quantitative RT-PCR analysis (mean±SEM) of *LONP1* in Hep3B (n=6 except for MeOH, Rot and TG n=7), U-251MG (n=6 except for EFV10 n=5, EFV25 and TG n=7) and HUVEC (n=6). (**E**) Analysis of the recruitment of NF-κB to the promoter of *LONP1*. Representative image of semiquantitative PCR after chromatin immunoprecipitation (ChIP) with anti-NF-κB; a non-related antibody anti-IgG and a sample of the input chromatin were used as controls. Aside from the aforementioned stimuli, cells were also treated with a proinflammatory stimulus a cocktail of LPS, IFN-γ and TNF-α, a known activator of NF-*k*B, which was employed as an additional control condition. (**F**) Study of ClpX expression by immunoblot in total cell extracts showing a representative image and a histogram of data quantification (mean±SEM, n=6). Results are expressed as % of control (untreated cells considered 100%). Statistical analysis was performed by One-way ANOVA ($^{*}P<0.05$ for EFV vs MeOH and $^{\#}P<0.05$ for TG, Rot or CCCP vs DMSO).

Fig. 5

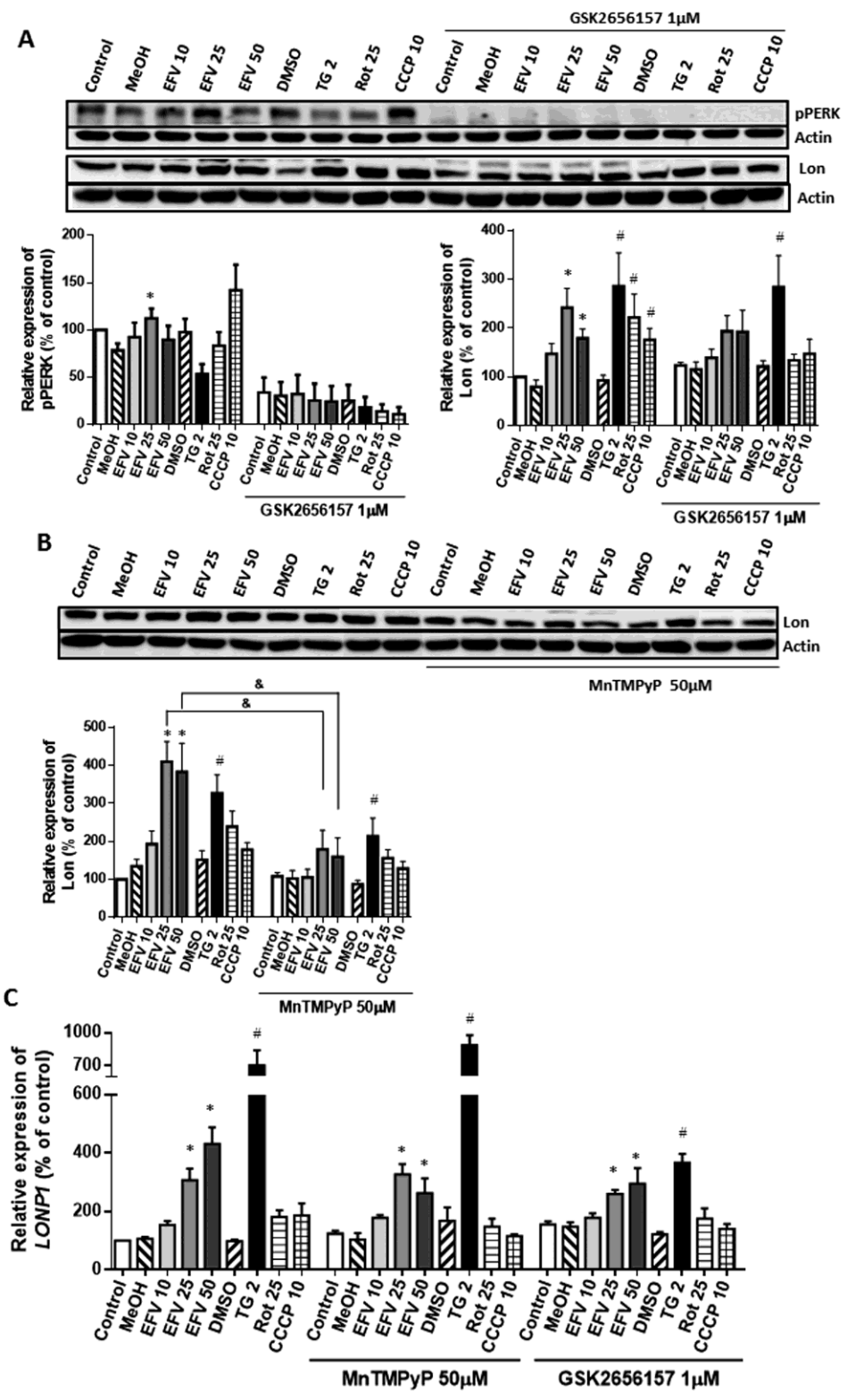

Fig.5. Analysis of the regulation of Lon´s expression. Cells were pretreated with the pPERK-inhibitor GSK2656157 or the catalase/SOD mimetic MnTMPyP for 1h and then treated for 24h with increasing concentrations of efavirenz (EFV), vehicle, thapsigargin (TG) 2µM, rotenone (Rot) 25µM or CCCP 10µM. (**A**) and (**B**) WB analysis of PERK phosphorylation and Lon

expression in whole cell extracts. Representative immunoblots and histograms of the data quantification are shown. (**C**) Quantitative RT-PCR analysis of *LONP1*. Results (mean±SEM) are expressed as % of control (untreated cells considered 100%); (A) left panel n=7 for cells without pretreatment and n=5 for pretreated cells; (B) n=5 and (C) n=9 for cells without pretreatment and n=5 for pretreated cells. Statistical analysis was performed by One-way ANOVA ($^{*}P<0.05$ for EFV vs MeOH and $^{\#}P<0.05$ for TG or Rot vs DMSO, and &P<0.05 for cells with vs those without pretreatment).

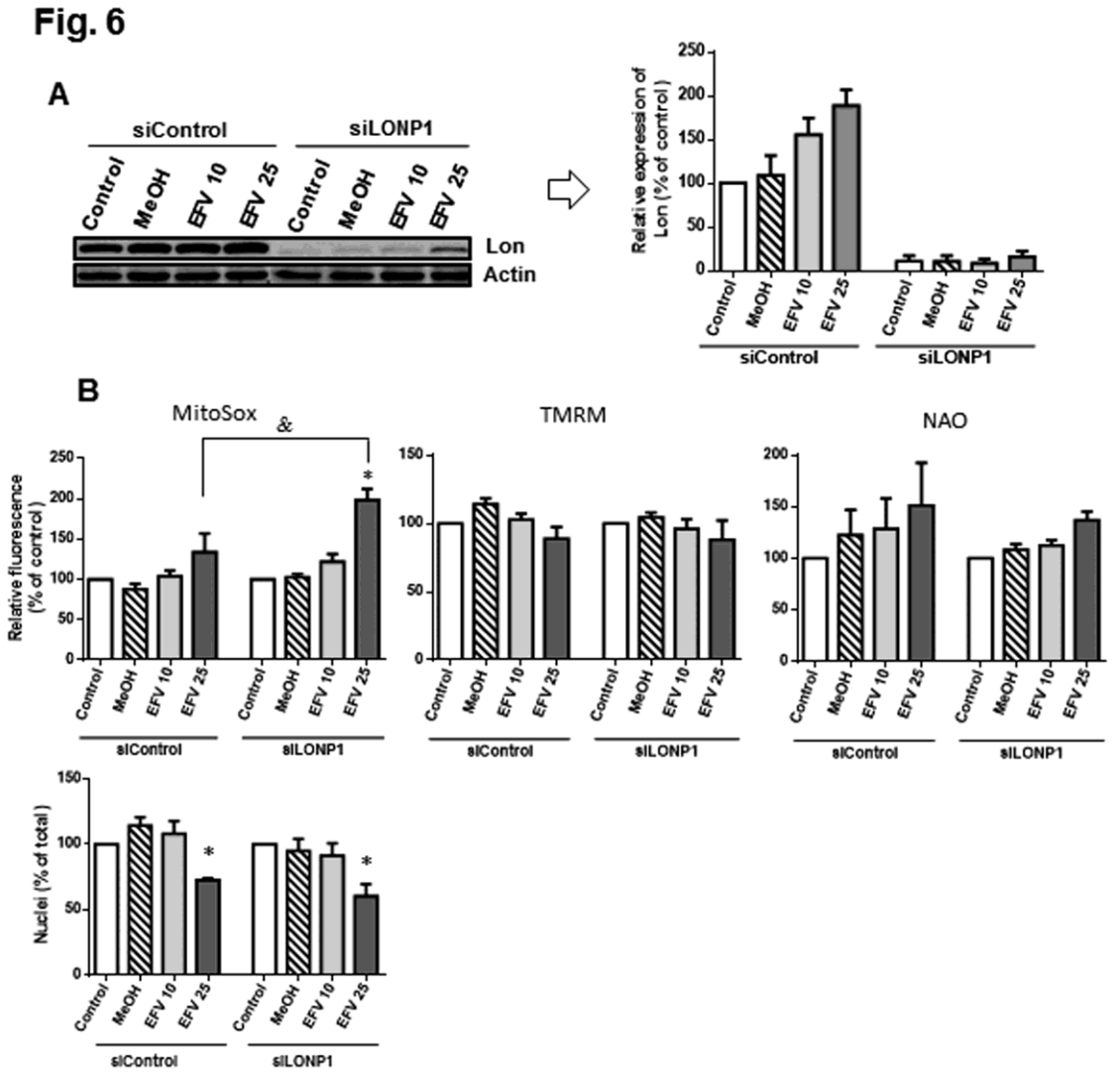

Fig.6. Analysis of Lon´s participation in the effect of EFV. Cells were transfected with siRNA Control or siLONP1 and treated for 24h with efavirenz (EFV) or vehicle (MeOH). (**A**) Representative WB image and histogram expressing quantification of Lon expression. (**B**) Histograms showing mean MitoSox (mitochondrial superoxide production), TMRM (mitochondrial membrane potential) and NAO fluorescence (mitochondrial mass) - upper panel) and number of nuclei (visualized with Hoechst fluorescence) - lower panel. Data (mean ± SEM, n=5 in (A) and in (B)-upper panel, and n=9 in (B)-lower panel) are expressed as % of control (considered 100%). Statistical analysis was performed by One-way ANOVA ($^{*}P<0.05$ for EFV vs MeOH).

Fig. 7

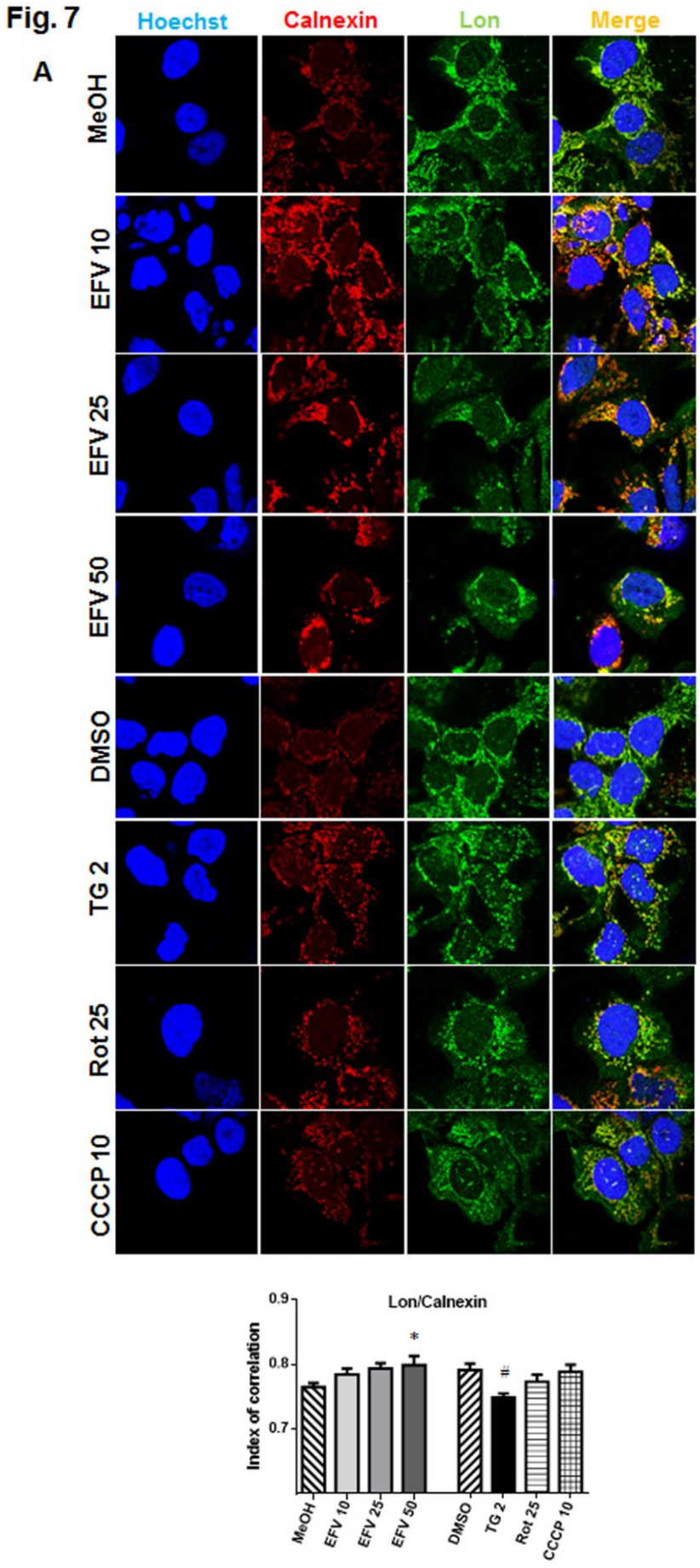

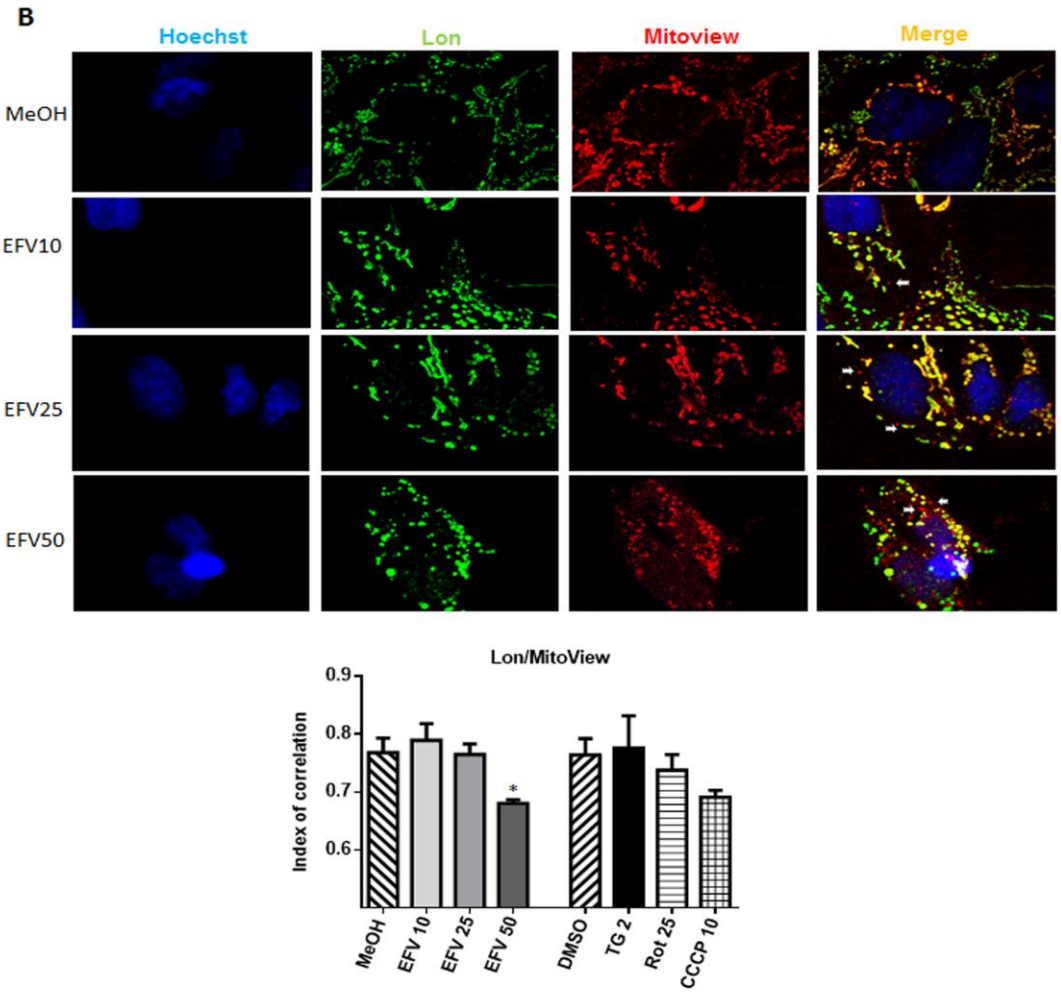

Fig.7. Analysis of Lon´s presence in ER and mitochondria by confocal microscopy. Cells were treated for 24h with increasing concentrations of efavirenz (EFV), vehicle, thapsigargin (TG) 2µM, rotenone (Rot) 25µM or CCCP 10µM, and stained with (**A**) Hoechst 33342 (nuclei), anti-Calnexin (ER) antibody and anti-Lon antibody or (**B**) Hoechst 33342 (nuclei), anti-Lon antibody and Mitoview (mitochondrial matrix fluorescent marker). Representative confocal microscopy images of 63x maginification with 3x optical zoom (A) or 3x optical+1.5x digital zoom (B), and a histogram showing the index of correlation between Lon and ER (A) and Lon and mitochondria (B). White arrows show mitochondria that do not overlap with Lon. Data are shown as mean±SEM, n=5. Statistical analysis was performed by One-way ANOVA ($^{*}P<0.05$ for EFV vs MeOH and $^{\#}P<0.05$ for TG, Rot or CCCP vs DMSO).

Fig. 8

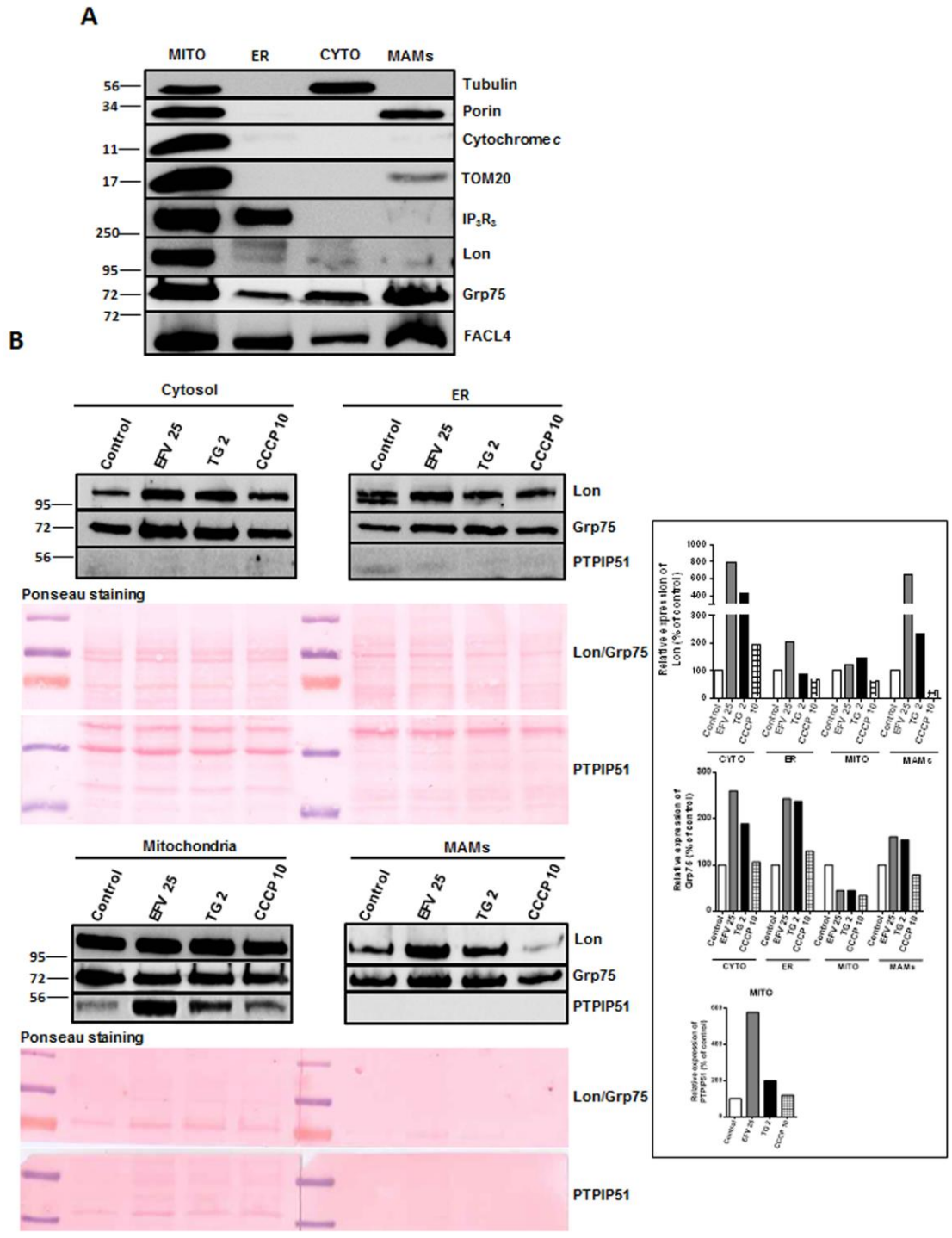

Fig.8. Analysis of the extramitochondrial expression of Lon. (**A**) Analysis of the purity of different cell fractions (mitochondrial, ER, cytosolic and MAMs) in untreated cells. Representative WB image showing the expression of several mitochondrial (Porin, Cytochrome *c*, TOM20, Lon), ER (IP_3R_3), cytosolic (Tubulin) and MAMs (FACL4, Grp75)

proteins in basal conditions. (**B**) WB analysis of Lon, Grp75 and PTPIP51 in cytosolic, ER, mitochondrial and MAMs fraction obtained in cells treated for 24h with efavirenz (EFV), thapsigargin (TG) 2μM, or CCCP 10μM. A representative experiment is shown, quantification data expressed as % of control (being the expression in the untreated cells in each fraction considered 100%). Ponceau staining of proteins was used as a loading control to normalize the results - equal relative amounts of protein load per lane in each extract.